Ventricular Rotation and the Rotation Axis

A New Concept in Cardiac Function

Ulf Gustafsson

Institution of Public Health and Clinical Medicine
Umeå University
Umeå 2010

Responsible publisher under swedish law: the Dean of the Medical Faculty

New series No. 1378
ISBN: 978-91-7459-096-8
ISSN: 0346-6612
Cover by Ulf Gustafsson
E-version avaible at http://umu.diva-portal.org/
Printed by: Print & Media
Umeå, Sweden 2010

This work is dedicated to
Anny and Nelli

Anny

Nelli

Table of Contents

Table of Contents ii
Abstract iv
List of papers vi
Abbreviations vii
Definitions viii
Enkel sammanfattning på svenska/ Summery in Swedish ix
Preface xii
Introduction 1
Cardiac cycle 2
Cardiac mechanics 3
Echocardiography 5
Speckle tracking 7
Assessing cardiac function 8
Statistical considerations 9
Aims 11
Methodology 12
Materials 12
Echocardiographic equipment 14
Image acquisition 14
Offline analyses 14
The rotation axis 16
Reproducibility and quality measures 18
Statistical analyses 18
Results 20
Left ventricular rotation 20
Regional rotation *20*
Untwist *21*
Right ventricular rotation 22
Segmental analysis *23*
The rotation axis 25
Method *25*
The rotation axis in healthy humans *25*
The transition plane *26*
Example of the rotation axis in a patient with reduced LV function *27*
The rotation axis in acute ischemia 29
Rotation axis at baseline *29*
Rotation axis during ischemia *29*
Stability of the rotation axis *31*
Rotation and twist *31*

AV-plane displacement *31*
Wall motion score *31*
Reproducibility and quality measures 32
Rotation *32*
Rotation axis *32*
Discussion **34**
Left ventricular rotation 34
Right ventricular apical circumferential motion 36
The rotation axis 37
Method *37*
Rotation axis in healthy humans *38*
Transistion plane *39*
Rotation and the rotation axis in acute ischemia 39
Limitations **42**
Left and right ventricular rotation 42
Rotation axis 42
Main Findings **43**
Conclusion **44**
Acknowledgements **45**
References **46**
Supplements **53**

Abstract

Background: The twisting motion of the left ventricle (LV), with clockwise rotation at the base and counter clockwise rotation at the apex during systole, is a vital part of LV function. Contraction of obliquely oriented myocardial fibres of the LV ventricle, which constitutes about 60% of the myocardium, creates the systolic twisting motion, with clockwise basal rotation and counter clockwise apical rotation. Even though LV rotation has been studied for decades, the rotation pattern has not been described in detail. By the introduction of speckle tracking echocardiography (STE) measuring rotation has become easy of access. However, the axis around which the LV rotates has never before been assessed. The aims of this thesis were to describe the rotation pattern of the LV in detail (study I), to assess RV apical rotation (study II), develop a method to assess the rotation axis (study III) and finally to study the effect of regional ischemia on the rotation pattern of the LV (study IV).

Methods: Healthy humans were examined in study I-III and the final study populations were 40 (60±14 years), 14 (62±11 years) and 39 (57±16 years) subjects, respectively. In study IV six young pigs (32-40kg) were examined while being sedated and under influence of negative inotropic drugs. Standard echocardiographic examinations were performed, recording the motions of the ventricles and intraventricular blood flow. In study II additional short axis images at the apical level of both LV and RV simultaneously were recorded to study interventricular differences in rotation. In study IV short axis images and apical four chamber images were recorded before and 4 minutes after occlusion of left anterior descending coronary artery (LAD). Rotation was assessed in short axis images by using a speckle tracking software. In each analysis, rotation was measured in six subdivisions (segments) of the circumference throughout the cardiac cycle. Timings of cardiac phases were assessed by measuring time to opening and closure of valves in Doppler recordings at inflow and outflow areas of the LV. Measurements of LV geometry was done at both end systole and end diastole to be used in calculations of rotation axes. Based on geometry and rotation data of the LV, planes with similar rotation along its circumference (rotation plane) were calculated at different levels of the LV. The rotation axis of the rotation plane represents the rotation axis of the LV at that specific level. Using this method, rotation axes were calculated at basal, mid and apical levels of the LV in every image frame throughout the cardiac cycle. Additionally, the transition plane, where basal and apical rotations meet, was calculated. In study IV, longitudinal displacement (AV-disp) and wall motion score (WMS) were also assessed.

Results: Study I showed significant difference in rotation between basal and apical rotations, as well as significant differences between segments at basal and mid ventricular levels, while homogenous rotation was found at the apical level. The rotation pattern of the LV was associated with different phases of the cardiac cycle, indicating its importance to LV function. Study II found significant difference in apical rotation between the LV and the RV. RV rotation was heterogenous and bi-directional, creating a "thightening belt action" to reduce it circumference. Study III indicated that the new method could assess the rotation axis of the LV with acceptable reproducibility, quality and high correlation to manual calculations. The motion of the rotation axes in healthy humans displayed a physiological pattern by being directed closer to the outflow in systole and back towards the inflow in later diastole. Study IV found a significant difference in the rotation pattern, between baseline and after LAD occlusion, by measuring the rotation axes, but not by conventional measurements of rotation. AV-disp and WMS were also significantly changed by inducing regional ischemia.

Conclusion: There are normally large regional differences in LV rotation, which can be associated with anatomy, activation pattern and cardiac phases, indicating its importance to LV function. In difference to the LV, the RV did not show any functional rotation. However, its heterogeneous circumferential motion could still be of importance to RV function and may in part be the result of ventricular interaction. The rotation axis of the LV can now be assessed by development of a new method, which gives a unique view of the rotation pattern. Quality measurements and the consistent rotation pattern in healthy humans indicate that the new method has a potential clinical implication in identifying pathological rotation. This was supported by the experimental study showing that the rotation axis was more sensitive than traditional measurements of rotation and as sensitive as AV-disp and WMS in detecting regional myocardial dysfunction.

List of papers

This thesis is based on the following papers. They are reffered to by their Roman numeral and the papers are in their full format included as appendices at the end of this thesis.

I. Assessment of regional rotation patterns improves the understanding of the systolic and diastolic left ventricular function: an echocardiographic speckle-tracking study in healthy individuals. Gustafsson U, Lindqvist P, Morner S, Waldenstrom A. *Eur J Echocardiogr* 2009;10:56-61.

II. Apical circumferential motion of the right and the left ventricles in healthy subjects described with speckle tracking. Gustafsson U, Lindqvist P, Waldenstrom A. *J Am Soc Echocardiogr 2008;21:1326-30.*

III. The rotation axis of the left ventricle - A new concept derived from ultrasound data in healthy individuals. Gustafsson U, Larsson M, Bjällmark A, Lindqvist P, A´Roch R, Haney M, Waldenström A. *Manuscript.*

IV. The effect of acute myocardial ischemia on the rotation axis of the left ventricle. Gustafsson U, Larsson M, Bjällmark A, Lindqvist P, A´Roch R, Haney M, Waldenström A. *Manuscript.*

Abbreviations

A, A-wave	Atrial filling
A-onset	Onset of atrial filling
AVC	Aortic valve closure
AVO	Aortic valve opening
CRT	Cardiac rezynchronization theraphy
CV	Coefficient of variation
E, E-wave	Early filling
E-end	End of early filling phase
E-peak	Peak early filling blood flow velocity
ECG	Electrocardiogram
IVC	Isovolumic contraction
IVR	Isovolumic relaxation
LAD	Left anterior descending coronary artery
LV	Left ventricle
MVC	Mitral valve closure
MVO	Mitral valve opening
Q-wave	First part of the QRS-complex in the ECG
ROI	Region of interest
RV	Right ventricle
STE	Speckle tracking echocardiography
WMS	Wall motion score

Definitions

Systole – Cardiac phase from onset of QRS in the ECG to AVC.

Diastole – Cardiac phase from AVC to onset of QRS in the ECG.

Twist – Simultaneously basal clockwise and apical counter clockwise rotation.

Untwist – Simultaneously basal counter clockwise and apical clockwise rotation.

Rotation line – a line between two points with similar rotation values in opposite ventricular walls in an apical long-axis view of the LV, where at least one point is located at either the basal, mid ventricular or apical level, see Figure 11.

Rotation plane – a three-dimensional plane constructed by three rotational lines originating from the same level, see Figure 11.

Rotation axis – the central normal vector of a rotation plane, i.e. the axis around which the LV rotates in a rotation plane, see Figure 11.

Transition plane – a rotation plane with rotation values close to zero.

z-level – the distance in percent between the apex and the mean z-coordinate (centre) of the transition plane, with 0% at the apex and 100% at the base.

Deflection – the angle between a rotation axis and the longitudinal axis of the LV, defined as $angle_{(z)}$ in Figure 11.

Direction – the direction of a rotation axis in the transverse plane of the LV, defined as $angle_{(xy)}$ with 0° at the lateral wall and increasing angles counter-clock wise, see Figure 11.

Twist-ratio – the ratio of apical rotation to sign-reversed basal rotation.

Weighted mean – the direction of the rotation axis weighted by the deflection of the rotation axis, see figure 8.

Enkel sammanfattning på svenska/Summery in Swedish

Inledning

Vänster kammares (VK) rotation har visats vara av betydelse för dess funktion. Den systoliska vridningen med motsols rotation i apex och medsols rotation i basen är starkt kopplad till ejektionsfraktionen. Återvridningen under diastole har även stor betydelse för fyllnaden av VK. Vridrörelsen uppstår genom kontraktion av sneda, helixformade muskelfibrer som finns både subendokardiellt och subepikardiellt i VK och utgör närmare 60% av myokardiet. Rotationsrörelse har tidigare varit svår att studera med ultraljudsteknik, men genom introduktionen av ”speckle tracking” inom ultraljud kan nu rotation analyseras med lätthet. Rotation analyserat med speckle tracking har visats vara tillförlitligt genom validering mot andra metoder. Trots omfattande studier om rotationen, dess funktion och betydelse för VK är den inte fullständigt utredd. Rotationsmönstret har inte beskrivits i detalj och ingen tidigare studie har beskrivit den axel VK roterar omkring (rotationsaxeln). Studier på regionalt nedsatt myokardfunktions påverkan på rotationen har visat varierande resultat, men indikerar på en begränsad möjlighet att identifiera regional dysfunktion i VK genom att studera rotation. Höger kammares rotation har betraktats vara av liten betydelse för funktionen, men dess rotationsmönster har sällan studerats och aldrig tidigare beskrivits med speckle tracking. Målsättningen med avhandlingen var att detaljerat beskriva VK rotationsmönster (studie I) och HK apikala rotation (studie II) samt att utveckla en metod för att beräkna VK rotationsaxel (studie III) och studera hur regional ischemi påverkar rotationsmönstret (studie IV).

Material och method

Friska, slumpmässigt utvalda individer användes i studie I-III och antalet individer efter exkluderingar var i respektive studie 40, 14 och 39 individer. Medelålder för respektive grupp var 60±14, 62±11 och 57±16 år. De hade ingen känd hjärtsjukdom, tog inga mediciner för hjärta eller blodtryck, hade normalt EKG och ett blodtryck under 160/90. I studie IV användes 6 unga grisar, 32-40kg som var sövda och påverkade av negativt inotropa droger vid undersökningstillfället. I samtliga studier gjordes en standardiserad ekokardiografisk undersökning där 2D-bilder av hjärtat registrerades från olika vinklar samt blodflöden till och från VK. I studie II studerades rotationsmöntret endast under systole och kortaxelbilder registrerades av både vänster och höger kammare simultant vid apikal nivå. I studie IV

gjordes registreringarna strax innan och 4 minuter efter att ischemi inducerats. Rotation analyserades med speckle tracking-teknik vid 3 nivåer i VK och vid apikal nivå i HK. Rotationsanalysen i varje kortaxelbild delades in i 6 segment och medelvärde av varje segment registrerades. För beräkning av rotationsaxlar mättes VK geometri vid slutdiastole och slutsystole. Tider av klafföppningar och stängningar mättes från Doppler-registreringar vid inflöde och utflöde i VK och tillämpades till andra hjärtcykler med liknande frekvens. Baserat på data av VK geometri och rotation beräknades plan med liknande rotationsvärden (inom 0,5°) mellan de olika väggsegmenten av VK. Rotationsaxeln för rotationsplanet representerar VK rotationsaxel vid samma nivå. På detta sätt kunde rotationsaxeln studeras vid olika nivåer i VK i varje bildruta under hela hjärtcykeln. Dessutom beräknades transitionsplanet, dvs den nivå med noll grader rotation där basal och apikal rotation möts. Rotationsmönstrets påverkan av regional dysfunktion studerades på 6 grisar genom att ockludera det främre neråtgående vänstra koronara kärlet (LAD) proximalt eller vid mid-nivå. Förutom rotation analyserades AV-plansrörlighet (AV-plan) och regional väggfunktion genom visuell bedömning (WMS) före och efter 4 minuter med ischemi.

Resultat

Studie I: Signifikanta skillander mellan basal och apikal rotation fanns vid alla uppmätta tidpunkter under hela hjärtcykeln. Vid basal och midventrikulär nivå var det signifikant mer medsols rotation i inferoseptala segmenten jämfört mot anterolaterala segmenten. Vid apikal nivå fanns det ingen signifikant skillnad mellan segmenten. Rotationen i VK kunde kopplas till olika händelser i hjärtcykeln. Studie II: Signifikant skillnad i apikal rotation fanns mellan VK och HK från 50% av ejetionstiden till slutsystole. HK uppvisade bidirektionell cirkumferentiell rörelse medan VK hade en homogen rotationsrörelse. Studie III: Den nya metoden kunde lokalisera rotationsplan med acceptabel reproducerbarhet, liten variation inom rotationsplanen och med mycket god korrelation mot manuella beräkningar. Rotationsaxlarna hos friska individer visade ett konsekvent rörelsemönster där axlarna riktades närmare utflödesdelen i systole och återgick mot inflödet i senare delen av diastole. Studie IV: Vid induktion av LAD-ocklusion sågs en signifikant respons i rotationsmönstret genom att studera rotationsaxlarna. Den tillkomna myokarddysfunktionen kunde inte signifikant bekräftas med traditionella mätningar av rotation, dock med AV-plansmätning och med WMS.

Konklusion

Vänster kammare har normalt stora regionala skillnader i rotation som kan kopplas till anatomi, aktiveringsmönster och olika faser i hjärtcykeln, vilket indikerar på dess betydelse för VK-funktionen. VK har en funktionell rotation som sannolikt är av betydelse för funktionen. HK uppvisade ingen funktionell rotation, däremot har dess heterogena cirkumferentiella rörelse sannolikt betydelse för dess funktion och kan delvis vara ett resultat av interaktionen mellan ventriklarna. Genom utvecklandet av en ny metod kan vi nu beskriva VK rotationsaxel vid flera nivåer och transitionsnivån där basal och apikal rotation möts. Hos friska individer sågs ett dynamiskt och fysiologisk rörelsemönster av rotationsaxlarna. Den nya metoden för att beräkna rotationsaxlar ger en unik bild över rotationsmönstret i VK. Spridningen, reproducerbarheten och kvalitetsanalyserna indikerade att den nya metoden kan vara användbar för att skilja mellan ett friskt och ett sjukt rotationsmönster. Rotationsaxlarnas orientering verkar vara ett känsligare mått än traditionella mätningar av VK-rotation och likvärdig som AV-planmätningar och WMS för att upptäcka regional dysfunktion. Fortsatta studier för att utvärdera metoden behövs för att se dess potentiella kliniska tillämpningar.

Preface

This thesis started out as an attempt to shed more light on the role of ventricular twist in cardiac function, by using the newly introduced speckle tracking technique. However, already during the first study of rotation in healthy humans, an unexplained consistent motion was detected. At the papillary level in the LV, a bidirectional rotational motion was seen, which puzzled our minds. This motion could only be explained by the fact that the LV does not rotate around its longitudinal axis (illustration below). Out of this the theory of the rotation axis was born.

Throughout the second study further development of the theory and the method of the rotation axis continued. After spending more than one year in development of software that calculates the rotation axis of the LV, with numerous improvements and adjustments of the software, finally a software version being more than 95% accurate was ready to be applied in studies. The development of the software was done in collaboration with two engineers at KTH in Stockholm, Matilda Larsson and Anna Bjällmark, who helped me beyond what any one could have asked for.

The process of developing a new method has learned me a lot. Being alone, facing all problems when trying to objectify our ideas without references has both been encouraging and frightening. It has also given me tremendous respect for those creating new methods. Even though this process has been testing my patience and challenged my mind, I'm glad to have chosen this route as my doctorial studies. Without the support from my head supervisor Anders Waldenström, who believed in my ideas from the very beginning, the development of the new method would not have commenced. These studies have led me from an innovating idea to a new clinical tool for evaluating cardiac function, of which I'm proud.

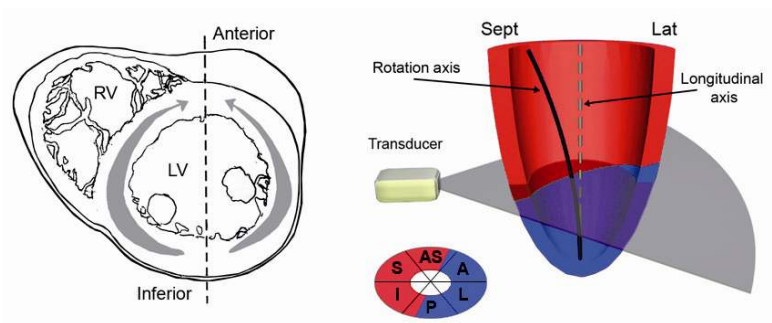

Introduction

Through time and evolution the human heart has evolved into a highly efficient pump, delivering more than 5000 litres of blood every day in a typical adult. This magnificent organ has a complex structure, which determines its special motion and has intrigued man through time. Two of the oldest medical notes about the function of the heart are the ancient Egyptian scrolls called Edwin Smith Papyrus and Ebers Papyrus, dated to 1600 BC and 1550 BC [1, 2]. The scrolls describe the heart as the central pumping force of the blood with descriptions of symptoms and treatment of cardiac diseases. However, to the ancient Egyptians the heart was associated with spiritual and mystical believes and they also thought that the heart was the centre of knowledge [2]. Three thousand years later, in the 15th century, the famous drawings and descriptions by Leonardo da Vinci gave detailed insight into the complex structure and function of the heart (figure 1) [3, 4]. Still, at the time of da Vinci, the general belief was that in the circulatory system blood was produced in the liver and consumed by the muscles [5]. The modern knowledge of the circulatory system was introduced by William Harvey in the beginning of the 17th century [6]. Later in the 17th century the function of the heart was described as ´the wringing of a linen cloth to squeeze out the water´ by Richard Lower, describing the twisting motion of the LV [7]. However, regardless of the importance of the twisting motion to cardiac function, focus has been on investigating the longitudinal and radial function of the ventricles, much due to the technical difficulties in measuring rotation. With the advancement of technologies and the introduction of speckle tracking in ultrasound imaging, it has now become easy to assess the rotational motion of the heart.

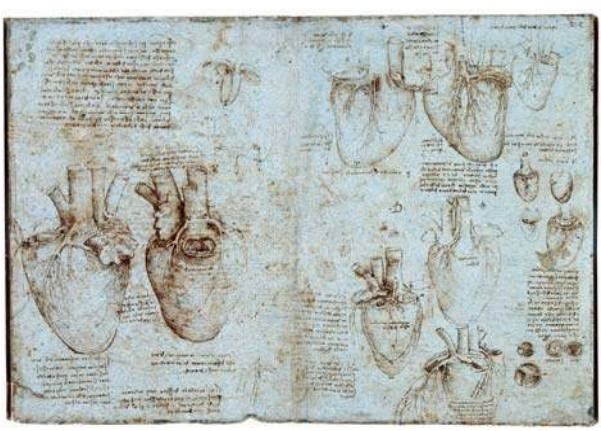

Figure 1. Anatomical drawings of the coronary vessels and the valves of the heart by Leonardo Da Vinci. The Royal Collection ©2010, Her Majesty Queen Elizabeth II.

Cardiac cycle

The cardiac cycle is divided in two periods, systole and diastole. During systole the ventricles of the heart pumps blood out in the body through the arteries. In diastole blood is filling the ventricles. The conventional definition of systole is the period between mitral valve closure (MVC) and aortic valve closure (AVC), with the rest of the cardiac cycle being diastole [8, 9]. In this thesis the systolic period is defined as the period between the onset of the R-wave in the ECG and AVC, as measurements of time were in reference to the onset of the R-wave. In normal conditions MVC occurs within 50-60 ms from the onset of the QRS complex [10-12].

The electrical activation of the ventricles, seen as the QRS-complex in the ECG, leads to contraction of the ventricles, rapidly increasing the intraventricular pressure. This initial period, when all valves of the heart are closed is called the isovolumic contraction (IVC). When the intraventricular pressures exceed the arterial pressures, the aortic and pulmonary valves open and the ejection of blood begins (figure 2). At end of ejection the aortic and pulmonary valves close, which mark the end of the systolic period.

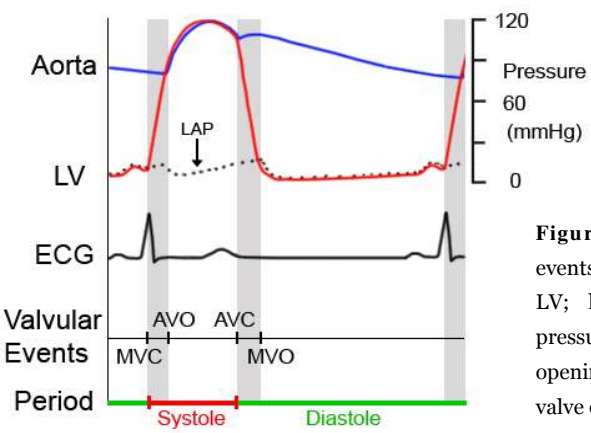

Figure 2. Pressures, ECG and valvular events during the normal cardiac cycle. LV; left ventricle, LAP; left atrial pressure, AVO/AVC; aortic valve opening/closure, MVO/MVC; mitral valve opening/closure.

The diastolic period represents the relaxation of the ventricles. The very first period of time in diastole is the isovolumic relaxation (IVR), which also is a phase when all valves of the heart are closed, during which the intraventricular blood pressure rapidly drops. When the intraventricular pressures are less than the pressure in the atria the atrioventricular (AV) valves open and the fast early filling (E-wave) of the ventricles begins. After the E-wave there is usually a period of slow filling, called diastasis, which ends when the atrias are contracting, lifting the AV-plane and driving blood into the ventricles (A-wave). After the A-wave, combined with the onset of

pressure increase of the ventricles, the AV valves close. This ends the diastolic period, completing the entire cardiac cycle.

Cardiac mechanics

The contractions of the ventricles are complex and elegant. Its structure provides auto-regulating mechanisms to maintain appropriate stroke volume and sufficient cardiac output [13]. The shortening of the contractile structures, sarcomeres, in the myocardium are about 15% in length, still the normal ventricle reduces its volume by approximately 60% [14]. The muscle fibres constituting the ventricular wall and their orientations are the key to the complex and highly efficient motion of the ventricles. The gross anatomy of the heart with its four chambers and valves is illustrated in figure 3.

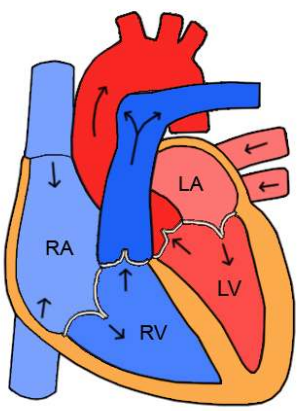

Figure 3. Gross anatomy of the heart. Red colour indicate oxygen rich blood entering the arterial system and blue colour indicate oxygen poor blood returning from the venous system. LA = left atrium, LV = left ventricle, RA = right atrium, RV = right ventricle.

The inner part of the LV wall, endocardium, consists of mainly longitudinal orientated fibres [15-17]. When contracting they shorten the length of the ventricle. In the subendocardial portion of the myocardium, between the endocardium and the middle layer of the ventricular wall, there are obliquely or helically orientated fibres in a right handed helix. The orientation of the subendocardial fibres turns progressively from the longitudinal orientation near the endocardium to a circumferentially orientation when approaching the middle of the myocardium (figure 4). Roughly at mid myocardium there are circumferential orientated fibres, mainly contributing to the radial shortening of the LV. The circumferential fibres are most pronounced at the base and become progressively less pronounced towards the apex. Between the circumferential fibres in the midwall and the outer part of the LV wall, epicardium, there are obliquely orientated fibres in a left handed helix (figure 5). At the epicardium there is a small portion of longitudinal orientated fibres. The obliquely orientated fibres constitute about 60% of the

myocardium and are responsible for creating the twisting motion of the LV [16-19]. The subendocardial oblique fibres, which have less mass than the subepicardial oblique fibres, are supposedly responsible for the untwisting motion of the LV in early systole [19-21]. During the rest of systole the subepicardial left handed fibres create the twisting motion of the LV, with basal clockwise rotation and apical counter clockwise rotation, as seen from the apex [22, 23].

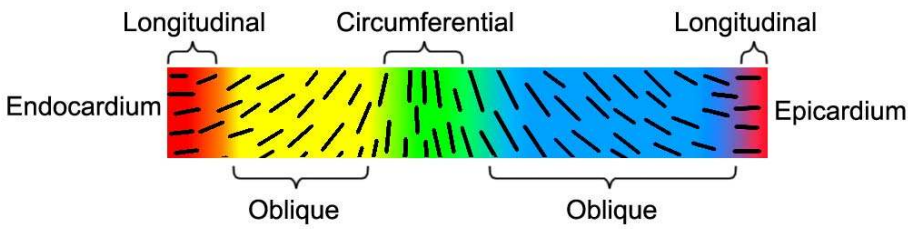

Figure 4. Illustration of the myocardial fibre orientation of the left ventricle from the endocardium to the epicardium. Colour codes; red = longitudinal fibres, yellow = oblique (right handed helix), green = circumferential, blue = oblique (left handed helix).

This structure with different fibre orientations across the ventricular wall gives the LV a pushing, squeezing and twisting motion to eject the blood. The combination of these motions during contraction allows the normal ventricle to reduce its volume by about 60% in every heart beat. The relaxation of the LV normally begins with untwisting at about the time of AVC and radial lengthening following closely, while longitudinal lengthening does not occur until close to MVO [23-26]. The lengthening is more rapid than the contraction in all dimensions, quickly reducing ventricular pressure and creating a suction effect that fills the ventricle with blood from the atria [27-29].

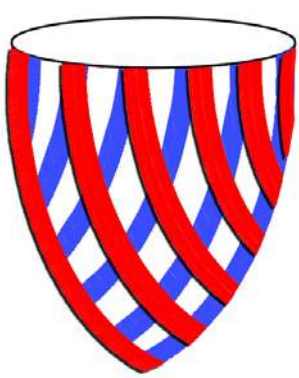

Figure 5. Illustration of the subendocardial right handed helix (blue) and the subepicardial left handed helix (red)

The RV consists mainly of longitudinally and circumferentially orientated fibres, constituting one endocardial 'layer' and one epicardial 'layer'. The endocardial layer of the myocardium mainly consists of longitudinally orientated fibres, while the epicardial layer mainly consists of circumferential fibres [15]. This is in contrast to the LV, which has a large portion of oblique fibres in between the longitudinal and circumferential fibres, creating a continuous and smooth transition from longitudinal to circumferential fibres resulting in no distinct separation of functional or anatomical layers. The RV primary works in a longitudinal and radial fashion to eject blood into the pulmonary vascular system. The RV has been so far less studied than the LV. Its longitudinal motion has been considered as the most important motion for its function [30, 31]. However, only a few studies on RV rotation or circumferential motion have been done and previously none by speckle tracking [32-34]. One other major difference between the ventricles is their configurations. The LV is formed like a rounded cone while the RV is crescent-shaped in short axis view, 'hanging on' to the LV. The shape of the RV results in a larger endocardial surface than the LV, which thereby requires less myocardial shortening than the LV to eject the same volume [13]. Another major difference is that the RV performs its work in an environment with much lower pressure that the LV. Several other differences between the ventricles exist, including the angle between inflow and outflow areas and the amount of trabeculation, which will not be further discussed in this thesis. However, the ventricles do not operate individually, but are dependent on each other. As the LV and the RV must produce the same volume over time to maintain balance between the systemic and pulmonary circulation, there must be mechanisms to regulate this. Studies have shown that the ventricles contribute to the each others efficiency [35-37].

Echocardiography

Assessing size, structures and function of the heart by ultrasound is today the most common method in clinical practise to evaluate cardiac function. Its combination of mobility, low cost and ability to view the structures and tissue non-invasively provides the healthcare with an attractive tool to easily address the question at hand in many situations. During the last two decades the use of ultrasound has advanced in healthcare and has surpassed other imaging techniques in some areas, one being cardiology. The value of magnetic resonance imaging, nuclear medicine and angiograms in cardiology is still recognised. However, for a basic evaluation of cardiac function and structures, echocardiography is today the first choice.

The basic concept of ultrasound imaging technology is simple, emission of sound and registration of the echoes from the emitted sound. The controlled

sound energy is produced by passing pulses of electricity through piezoelectric crystals which then vibrate and thereby generate sound waves. In the interval between the pulses of electricity, the returning sound waves of the echo makes the crystal vibrate and thereby generate electricity, which is registered. The echoes arise when a sound wave passes from one medium to another which has different acoustic impedance. This interface between media reflects part of the sound wave. The amplitude of the echo depends on how great the difference in acoustic impedance is between adjacent media. Blood, bone, muscle etc, has different acoustic impedance and within tissues, for instance the myocardium, there are structures with different acoustic impedance creating a variety of echoes. Using the information in the echo, amplitude and time, an image of the structures reflecting the sound can be constructed. Modern ultrasound machines typically generate between 40-70 (but also up to over 100) 2D images per second, making the temporal resolution high. When sound reflects by a structure in motion, the frequency of the sound is shifted. This is called the Doppler effect. By calculating shifts in frequency, the velocity of moving structures, such as blood or tissue, can be assessed. One common way to make practical use of the Doppler effect is to visualize and measure blood flow within the heart and major blood vessels, which adds information to the assessment of the function of the heart and valves.

The routine examination in echocardiography includes assessing size and function of ventricles, as well as the size of the atrias and the function of the valves. By generating 2D images, which is the most common method in echocardiography, single 'slice' images of the heart can be viewed from different angles and perspectives (figure 6). Special applications are used to measure dimension, motion and blood flow, from gray scale images, M-mode and Doppler recordings. The echocardiographic exam provides an overview of the heart and its function. However, detailed studies of morphology can also be done when image quality is high. One drawback of echocardiography is the user dependency, as the expertise of the operator can affect both the image acquisition and the interpretation of the images.

Figure 6. Standard echocardiographic images of the heart. From left to right; parasternal longaxis, parasternal short axis and apical four chamber images.

Speckle tracking

Speckle tracking echocardiography (STE) is a technique that enables angle independent measurements of motions in images, unlike traditional ultrasound which is angle dependent. With the introduction of this technique in echocardiography, assessing the function of the heart has in some aspects become easier, including for instance assessment of the rotational function of the LV. The STE technique estimates motions by tracking of speckles in the image. Speckles are the result of the acoustic noise generated when sound waves scatter in tissues. This phenomenon appears when sound waves are reflected by structures smaller than the wavelength of the sound. This causes the sound to scatter. Interference between echoes from different scatters either enhance or reduce each other [38]. This results in spatial fluctuations of the intensity in the image (Figure 7). As most structures causing scattering of the sound are stationary within the tissue, the speckles are fairly stable and highly related to myocardial motion [38, 39]. In the speckle tracking analysis, regions of speckles (kernels) are identified from frame to frame. The distance and direction one specified kernel has travelled over time can then be calculated (figure 7). Thereby the motion of the tissue can be assessed and presented as velocities, strain, rotation etc. STE has been validated against different methods and proven to be a reliable analysing tool for motion of tissue [38-40].

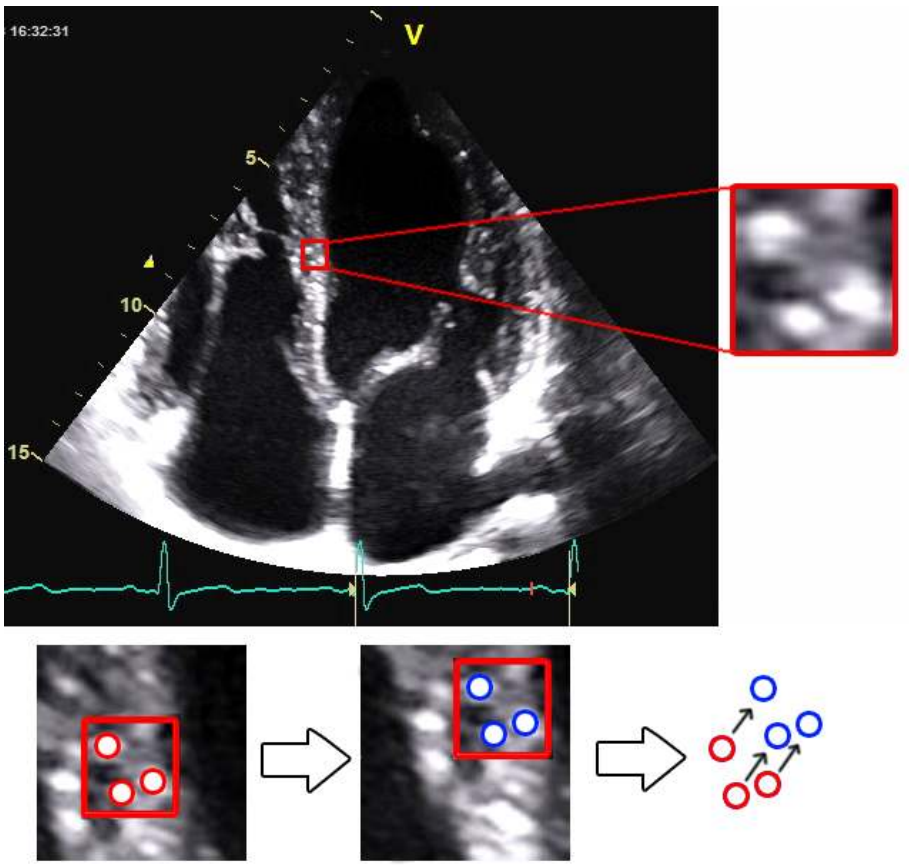

Figure 7. Example of the method of speckle tracking. Speckles are acoustic markers generated by the interference of the sound waves reflecting from the tissue (upper part). Formations of speckles (kernels) are identified in every frame making it possible to calculate motion (lower part).

Assessing cardiac function

Assessing cardiac function in clinical practice usually means assessing longitudinal and radial functions, not rotational function. Many different methods to assess longitudinal and radial function exist, displacement, velocities, strain, strain rate etc using 2D images, M-mode, tissue Doppler and speckle tracking. Assessing rotational function has been limited to measuring rotation and rotation rate by the use of offline speckle tracking analyses and to some extent tissue Doppler with the angular limitations of a one-dimensional technique. One common method of assessing regional function is by wall motion score, which performed qualitatively through a

subjective evaluation of wall motion. The accuracy of this method is obviously limited, since the result depends on the expertise of the observer. There is a need for an easily applied objective clinical tool for assessing myocardial function, both global and regional function, to further standardize evaluation of cardiac function.

Statistical considerations

In this thesis there are two types of data used, linear and circular. Linear data is ordered from 1-∞, while circular data is ordered between 0-360°. Analysis of linear data is common and many different methods are available. In circular statistics there are limited available methods. When combining circular and linear data the available statistical methods are further limited. Only the mean (weighted mean) of circular and linear data could be calculated, no variation or standard deviation, when using the statistical software of choice in this thesis. Comparison between groups could not either be calculated when combining circular and linear data. As the rotation axis of the LV is calculated and presented as deflection (linear data) and direction (circular data) at different levels of the LV, these issues were present. This is a methodological limitation in study III and IV. Hopefully, a solution to this problem is imminent.

Calculating the variables of the rotation axis independently generates different results than if calculated as the weighted mean. Deflection will be greater as all values are absolute. The direction of the rotation axis can also differ when calculated separately compared to weighted mean (figure 8). As the orientation of the rotation axis is determined by both direction and deflection, the most accurate way to present this is by the weighted mean. This limitation, not being able to statistically analyse some of the results other than when calculating the variables separately, is why both ways are used in study III and IV.

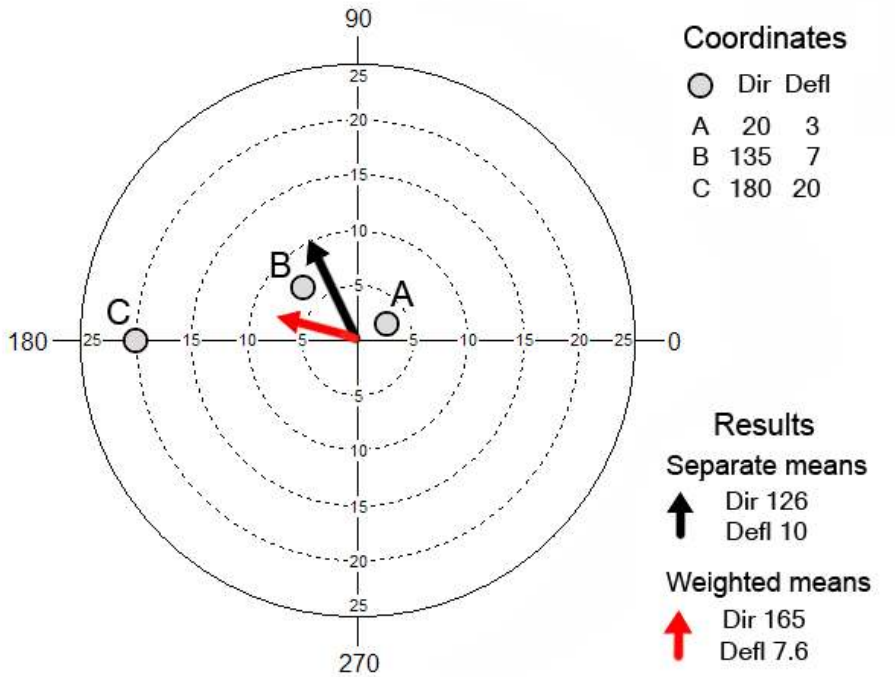

Figure 8. Example of the difference between calculating mean deflection (defl) and mean direction (dir) separately or combined as weighted mean. Calculating the mean of the three values (coordinates) of deflection and direction separately results in higher degree of deflection and less degree in direction (black arrow) than calculated as weighted mean (red arrow). Deflection is presented on the axial scale as the distance from the centre. Direction is presented by the circular scale (0-360°).

Aims

The general aim of this thesis was to characterise the relationship of ventricular rotation to function by using STI technique. This required the development of new methodology to present a coherent assessment of rotational function. Finally, evaluation of our new method in a clinically relevant experimental setting was needed.

Study I

To investigate the normal physiology of left ventricular rotation by studying the rotation pattern in detail in healthy humans.

Study II

To investigate whether RV apical rotation could be of importance in RV function and compare this with LV apical rotation.

Study III

To study the left ventricular rotation axis in healthy humans and to develop a method for quatification of the rotation axis.

Study IV

To study the effect of acute regional ischemia on the rotation axis of the LV and compare the results to other methods of measuring LV function.

Methodology

Materials

Study I. Forty healthy subjects (18 men), mean age 60 ± 14 (23 - 81) years, randomly selected from the local population list at the Swedish tax bureau were included. None had any history of hypertension or cardiac disease and were not taking any medication. All had normal ECG and a blood pressure below 160/90. Basic characteristics are presented in table 1. The study was approved by the local ethics committee and all subjects gave informed consent to participate.

Study II. The study population was a subgroup of the material in study I. In 30 subjects an attempt to record both ventricles simultaneously at the apical level was done. However, 16 subjects were excluded due to failure to simultaneously visualize both ventricles with good image quality. The remaining study population consisted of 14 subjects (8 men, mean age 62 ± 11 years (46 - 81 years).

Study III. The original study population consisted of 43 healthy subjects, the vast majority (40 subjects) were randomly selected from the local population list at the Swedish tax bureau. These 40 subjetcs were included in study I. Four subjects were excluded because they could not be analysed by the rotation axis software, due to inadequate tracking quality in the speckle tracking analysis. The final study population consisted of 39 subjects (20 men, mean age 57 ± 16 years). In addition, one patient with dilated cardiomyopathy was examined to test the method in a case of reduced rotational function. The function of the patients LV was clinically assessed as with general hypokinesia and anteroseptal akinesia and with an ejection fraction less than 30%.

Study IV. Six healthy juvenile Swedish landrace pigs, 32 - 40 kg, were studied under anaesthesia. At the time of the recordings the pigs were in good resting condition and on negative inotropic drugs (metoprolol and verapamil). The animals were anesthetised with intravenous barbiturate, opiate and benzodiazepine, tracheotomised and normoventilated. Arterial, central venous and pulmonary artery pressures were monitored as well as ECG, as described in an earlier study by A´Roch et al [41]. The study was conducted with approval of the local animal research ethics committee.

Tabel 1. Basic characteristics of the study population in study I.

Variable	*All subjects*	*Women*	*Men*	*P value*
Number	40	22	18	
Age (years)	60±14	60±14	61±14	0.770
Heart rate (bpm)	63±7	63±7	62±7	0.622
SBP (mmHg)	136±18	133±31	139±16	0.341
DBP (mmHg)	84±10	81±10	87±9	0.047
LV diastole (mm)	51±4	49±4	53±3	0.011
LV systole (mm)	33±4	32±4	35±4	0.033
IVS diastole (mm)	10±2	10±2	11±2	0.005
LVPW diast (mm)	8±1	7±1	8±1	0.011
LA (mm)	38±5	36±4	40±6	0.033
E/A ratio	1.1±0.4	1.1±0.3	1.1±0.5	0.921
AV-disp (mm)	13±1	13±2	13±2	0.639
Q-AVO (ms)	86±9	85±10	86±8	0.709
Q-AVC (ms)	389±21	396±21	380±18	0.011

Means ± standard deviation. SBP - systolic blood pressure, DBP - diastolic blood pressure, IVS - inter ventricular septum, LV – left ventricle, LVPW - left ventricular posterior wall, LA - left atrium, AV-disp – mean longitudinal peak displacement of AV-plane at four sites. Q-AVO – time from the Q-wave in ECG to aortic valve opening (by Doppler). AVC- aortic valve closure. E/A – mitral early wave/mitral atrial wave from Doppler signal. P value denotes differences between men and women.

Echocardiographic equipment

In all studies the echocardiographic images were recorded using the Vivid 7 Dimensions, ultrasound machine (Vivid 7, GE Healthcare, Horten, Norway) (figure to the right). During the first two studies version 5.1 was used and in study III both version 5.1 and 6.1.2 were used. In study IV version 6.1.2 was used. In study I-III the 4S probe was used in a harmonic imaging mode with a frequency of 1.7/3.4 MHz. Study IV was conducted with a M4S probe using the same frequency. Offline analyses were made using EchoPac PC (EchoPac, GE Healthcare, Horten, Norway). Study I and II were analysed using version 5.1.1 and study III and IV using version 6.2 of EchoPac PC.

Image acquisition

In study I-III standard echocardiographic images and Doppler signals were recorded according to recommended guidelines [42, 43]. Extra attention on aquiring images of high quality was given when recording short axis images. In study IV the recordings were done as similar as possible to a standard human echocardiographic examination. However, due to differences in anatomy, especially the shape of the thorax and orientation of the heart, images from an apical view were usually limited when examening pigs [44]. During the ischemia in the pigs, only short axis and apical four chamber images and blood flow at mitral and aortic valves were recorded. Short axis images of the LV were not any more difficult to record in pigs than on humans. In all studies the short axis images were recorded at a frame rate between 64 - 82Hz.

Offline analyses

All measurements of dimensions, M-mode and Doppler recordings were analyzed in EchoPac according to recommended guidelines [42, 43]. Assessment of wall motion score (WMS) in study IV was performed by an experienced examiner, blinded to the study design. Rotation analyses were done in 2D-

strain, an application in EchoPac. In the rotation analyses of the LV, the region of interest (ROI) was set from the inside of the endocardium and to cover most of the myocardium, along the circumference (figure 9). Care was taken not to include the pericardium in the ROI. When analysing rotation of the RV, the ROI was set only to include part of the interventricular septum, beside the myocardium of the free wall. The ROI was divided in 6 equally sized segments and rotation data for each segment was calculated. The reference image in the rotation analyses was set at end of systole. However, exceptions were made when tracking quality was insufficient.

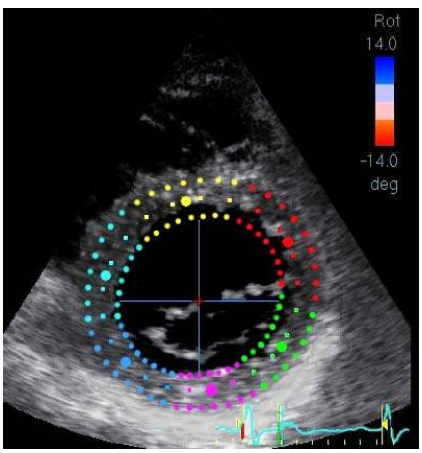

Figure 9. The region of interest (ROI) in a short axis image of the left ventricle. The ROI is set between the enodcardium and close to the epicardium. The six segments of the ROI are colour-coded differently.

Timings of valve openings and closures were measured in pulsed Doppler recordings at the valves (figure 10). The timings of the mitral blood flow were also measured in pulsed Doppler recordings. All time measurements were made in reference to the superimposed ECG, starting at the beginning of QRS. The individual timings of valves and mitral flow events were used as references in the rotation analyses as well as in the M-mode analyses. All rotation analyses were manually set to begin and end at the beginning of the QRS-complex to match the timings measured in Doppler recordings.

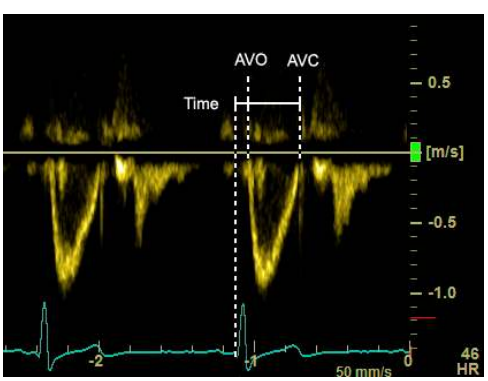

Figure 10. Doppler recording of blood flow at the left ventricular outflow tract. Illustration of the method to measure timings of aortic valve events. AVO/AVC = aortic valve opening/closure.

The rotation axis

The rotation axis method is designed to assess the axis around which the LV rotates. By finding equal rotation values at each of the six wall segments of the LV, a three-dimensional rotation plane can be estimated between the positions of these rotation values. Thereby, the normal axis of the rotation plane represents the rotation axis of the LV at that specific level.

From the rotation analyses by STE, the rotation value in each segment at basal, mid and apical levels are exported into text files. These files are then imported into custom made software that calculates the rotation axis. In addition to rotation values, end systolic and end diastolic diameters at each level and the distance from the apex to each level and time to end systole is added in the calculations. The geometric data is used to create an individual model of the LV upon which the rotation data is sampled (figure 11). The change in geometry over time is considered by linear interpolation between end diastolic and end systolic diameters. The rotation values are linearly interpolated longitudinally, every 0.1 mm from basal to mid level and from mid to apical level. This generates approximately 3000 coordinates with rotation data in every image frame throughout the cardiac cycle. The extent of rotation coordinates allows for detailed description of the rotation axis where even minor changes can be detected. If rotation values are missing, from the STE analysis, in maximum two out of the six segments at each level, rotation values are added to fill these gaps of data by linear interpolation between the adjacent segments. If data in three or more segments are missing, all data are excluded and no analysis of the rotation axis is performed. The software then searches for almost identical rotation values (< 0.05°) in opposite walls, always starting at one of the measured values at basal, mid or apical levels. If no value can be located within 0.05° at the opposite wall the software expands the search width to 0.5°. If still no matching rotation value can be found in the opposite wall, the software considers this as a missing value. When two almost identical rotation values (within 0.5°) are found in opposite walls, they form a rotation line with two coordinates describing its position (figure 11). This procedure is done between all three pairs of opposing walls (anteroseptal-posterior, anterior-inferior, septal-lateral) creating 3 rotation lines at each of the 3 levels (basal, mid and apical). The 6 coordinates of the 3 rotation lines originating at the same level is then condensed into 3 coordinates by calculating the mean coordinate for three pair of walls, anteroseptal-anterior, lateral-posterior and inferior-septal. These final 3 coordinates, at each level, define a rotation plane. From this rotation plane, the normal vector (90° to the plane) is calculated in reference to the longitudinal axis (figure 11). The result is presented as deflection and direction of the normal vector (rotation axis) at

all three levels. In addition, the transition plane is also calculated in a similar way. The transition plane describes the level in the LV where basal and apical rotations meet, where there by definition is zero degrees rotation. The position of the transition plane is calculated as percentage of the distance between the apex and the basal level. The deflection and direction of the normal vector to the transition plane is also calculated.

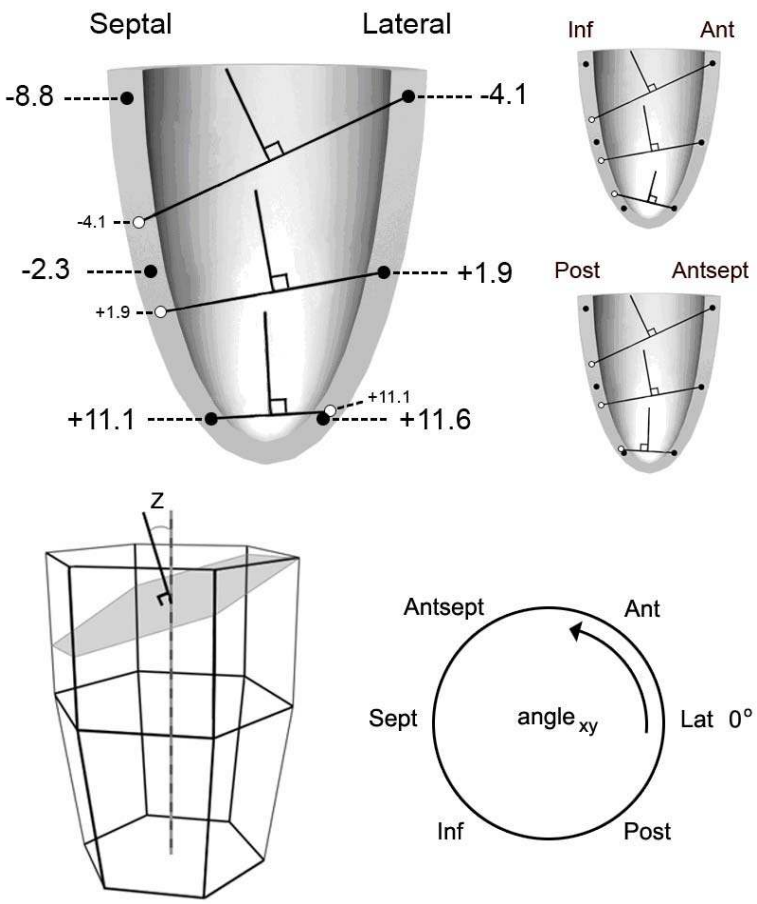

Figure 11. Schematic description of the calculation of the rotation axis. The upper illustrations show the LV from three apical long-axis views. The black filled dots represent segments with measured rotation values, the unfilled dots represent their matching rotation value (by interpolation) in the opposite wall. Rotation lines are defined as black lines between matching rotation values in opposite walls. To the lower left is the primary geometric model based on 18 coordinates (intersections of lines). The grey area represents the rotation plane. The deflection (Z, $angle_z$) of the rotation axis is relative to the longitudinal axis of the LV. The direction of the rotation axis ($angle_{xy}$) is presented in a circular scale (0° at the lateral wall and increasing angles counter clock wise), as illustrated to the lower right. Ant, anterior; Lat, lateral; Post, posterior; Inf, inferior; Sept, septal; Antsept, anteroseptal.

Reproducibility and quality measures

Rotation

All reproducibility tests of rotation were done measuring peak rotation at basal and apical levels. The inter-observer reproducibility test was done in the same rotation analysis in 5 randomly selected subjects. One intra-reproducibility test was done several weeks after the original analyses by re-analysing the images using the same ROI settings in 15 randomly selected subjects. Another reproducibility test was done by drawing a new ROI and re-analysing rotation in 6 randomly selected subjects.

Rotation axis

All reproducibility and quality measures were based on 10 randomly selected subjects included in study III. Mean deviation of the 6 rotation values constituting a rotation plane was calculated, as well as the number of frames in which no rotation plane could be calculated at every level. Another set of rotation data in each subject was created by re-analyzing the echocardiographic images by speckle tracking. Validation of the custom made software against visually estimation of the deflection and direction of the rotation axis was also done. The visual estimation of the rotation axis was done by using a sketched model of three different long axis views of the LV, as in figure 11, and assessing rotation lines. The combination of the rotation lines made it possible to estimate both deflection and direction of the rotation axes. The LV geometry and change of dimensions over time was not considered when visually estimating the rotation axis.

Statistical analyses

Study I. Mean and standard deviation were used to describe a central tendency and variation. SPSS 11.5 was used (SPSS, Inc., Chicago, IL). Repeated measurements ANOVA and post hoc paired t-test was used to compare levels. Repeated measurements ANOVA and post hoc paired t-test with Bonferroni correction was used to compare segments at each level at each time. Sampled paired t-test was used to compare time to peak rotation between apical and basal levels and the untwist amplitude between apical and basal levels. Independent t-test was used to compare peak rotation and time to peak rotation at apical and basal levels based on gender. Correlation between E and A velocities and untwist amplitude during E-wave and A-wave at basal and apical levels were analysed using Spearman´s correlation test. Inter- and intra observer reproducibility were analysed according to

Bland and Altman´s method of agreement and presented as the coefficient of variation (CV) [45].

Study II. Data are presented as mean ± SD and was analysed using the statistical software SPSS 14.0 (SPSS, Inc., Chicago, IL). Wilcoxon´s test was used to compare mean rotation at each time point and corresponding segments at AVC between the RV and the LV.

Study III. For all circular statistics Oriana 3 (Oriana 3, Kovach Computing Services, Isle of Anglesey, Wales, UK) was used. Mean, SD and 95% confidence interval of the direction of the rotation axis were calculated in Oriana 3. Rayleigh test was used to test uniformity in direction of the rotation axis. Mean, SD and 95% confidence interval of the deflection of the rotation axis were calculated in Excel (Microsoft Corporation, Redmond, USA). Reproducibility of the z-level of the transition plane and the deflection of rotation axes at all levels were calculated using the method of agreement as described by Bland and Altman and presented as the coefficient of variation (CV). The same method was used to calculate CV of the estimated and calculated z-levels of the transition plane and the deflections of the rotation axes at all levels. The reproducibility of the direction of the axes was assessed by testing the correlation between the two repeated measurements using the Oriana 3 software. The same correlation analysis was performed between the subjectively estimated direction and the calculated directions. Cubic regression was applied to demonstrate the relationship between the z-level of the transition plane and the LV twist-ratio.

Study IV. All circular statistics were calculated using a statistical program for circular statistics, Oriana 3. Rayleigh's test was used to identify significant mean directions of the rotation axis. Watson Williams F-test was performed to test differences in direction of the rotation axis between baseline and after LAD occlusion. Linear statistics were calculated using a statistical program (PASW Statistics 18, SPSS Inc. Chicago, IL). Wilcoxon signed rank test was used to test differences in deflection of the rotation axis, twist, rotation, timings, AV-plane displacement and WMS between baseline and after LAD occlusion. Stability of the rotation axis was calculated, defined as the mean of the differences in direction of the rotation axis between each measured time point in the interval from 75% ejection to MVO.

P-values less than 0.05 were considered as statistical significant in all studies.

Results

Left ventricular rotation

Of all analysed segments, 86% fulfilled the quality criteria in the analysing software. The following results are based on these successfully analysed segments. The basal level displayed a clockwise systolic rotation meanwhile the apical level rotated counter clockwise (figure 12). At AVC, which occurred at 389 ± 21 ms, the twist was 17.6 ± 5.3°. Peak basal rotation was 6.6 ± 4.5° at 377 ± 47 ms and peak apical rotation was 12.5 ± 4.8° at 391 ± 47 ms. There was no significant difference in time to peak rotation between basal and apical levels. At all time points there was a significant difference ($p<0.01$) between mean rotation at all three levels, except at 25% of ejection and at Q from the analyses of two heart cycles.

Regional rotation

In order to simplify, only comparison between opposite segments are presented as they most likely in general display the greatest differences between segments. At any level at any time point there was no significant difference between the anteroseptal and the posterior segments. At the basal level the inferior and septal segments rotated significantly more clockwise than the anterior and lateral segments during most of systole and part of diastole ($p<0.05$). At the papillary level a similar rotation pattern as at the basal level was seen (figure 13). The inferoseptal segments rotated significantly more clockwise than the anterolateral segments which rotated counter clockwise during most of the ejection phase and early diastole ($p<0.05$). Only at AVO there was a significant difference between the anterior and inferior segments at the apical level. No other significant differences between opposite segments were found at the apical level.

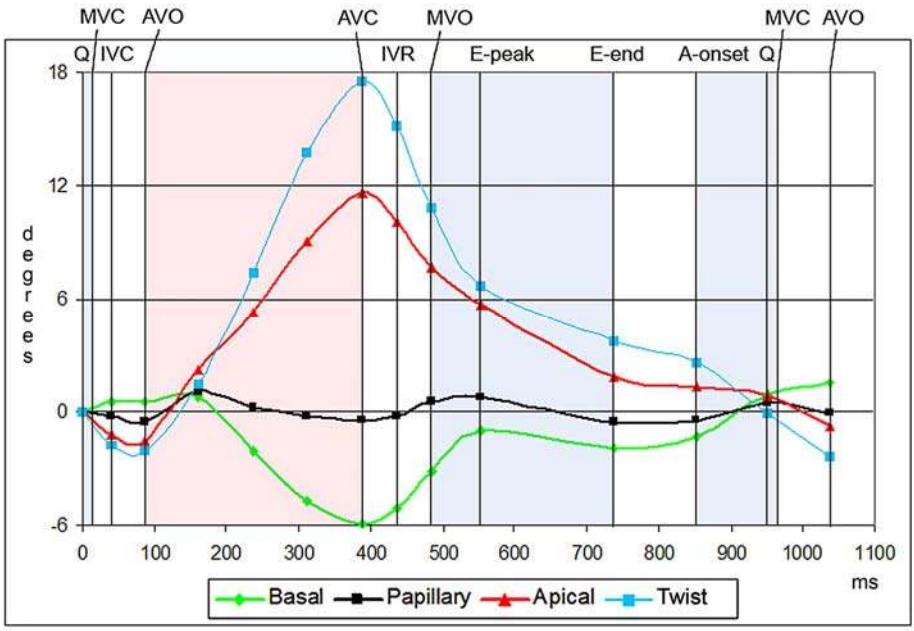

Figure 12. Mean rotation at each level and twist as the net difference between the apical and basal level over an entire heart cycle including the transition from diastole to systole in 40 healthy subjects. Q=Q-wave in the ECG, MVC=mitral valve closure, IVC=mid isovolumetric contraction, AVO=aortic valve opening, AVC=aortic valve closure, IVR=isovolumetric relaxation, MVO=mitral valve opening, E-peak=peak of early diastolic filling, E-end=end of early diastolic filling, A-onset=onset of late diastolic filling.

Untwist

At both filling phases, E and A, there was a significant difference in untwist ($p<0.001$). During the E-wave the apical untwist was more pronounced than the basal untwist (5.8 ± 4.9° and 2.0 ± 2.2° respectively). The early basal untwist ended at peak E while the early apical untwist ended at the end of the E-wave (figure 12). A significant correlation between E velocity and untwist during the E-wave was found at both the basal ($r = 0.340$, $p<0.05$) and the apical level ($r = 0.363$, $p<0.05$). Basal untwist during the A-wave was greater than apical untwist (1.9 ± 1.8° and 0.4 ± 1.5° respectively). There was no significant correlation between A velocity and untwist amplitude during the A-wave.

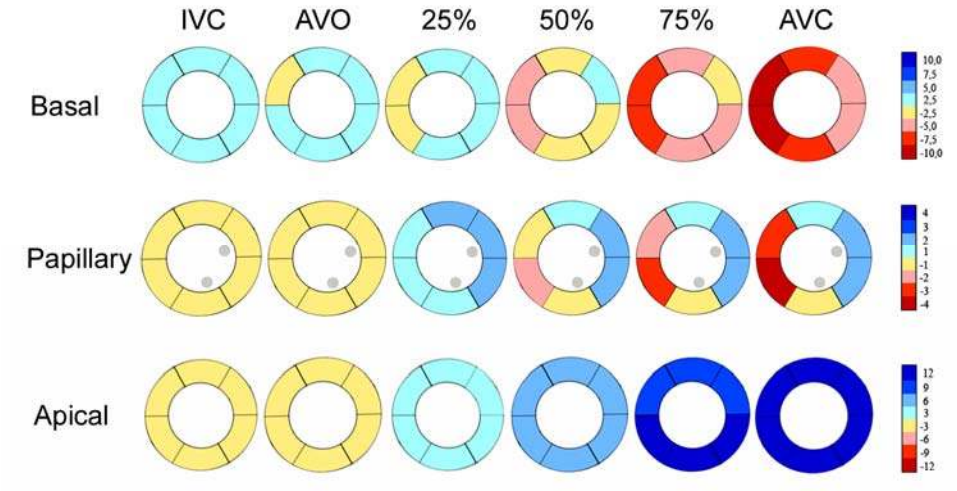

Figure 13. Colour coded mean segmental rotation at basal, papillary and apical levels of the left ventricle during systole in 39 healthy subjects. IVC = isovolumic contraction, AVO/C aortic valve opening/closure, 25% - 75% of ejection time.

Right ventricular rotation

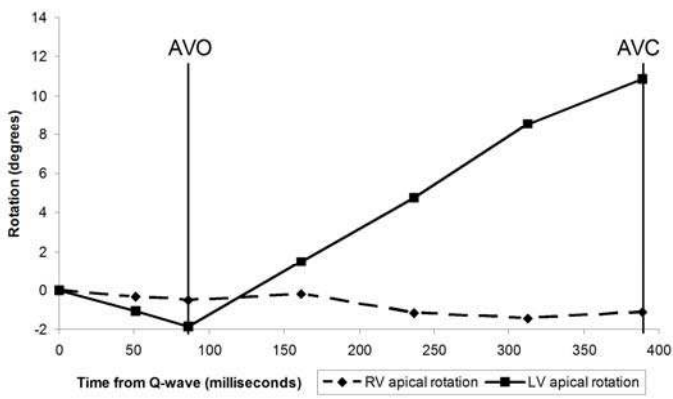

Figure 14. Mean rotation of the left and the right ventricle in 14 healthy subjects. AVO = aortic valve opening. AVC = aortic valve closure.

Of the analysed segments of both the left and the right ventricles, 95% were accepted by the quality criteria in the analysing software. There were only small differences in time to start and time to end of the ejection period between the left end the right ventricles (88 ± 10 ms vs 84 ± 8 ms and 390 ± 25 ms vs 393 ± 22 ms respectively). During the pre-ejection period there was almost no global rotation of the RV, in difference to the LV which rotated 1.7 ± 1.7° clockwise (figure 14). From the start of ejection the rotational direction of the LV changed to counter clockwise and maintained counter clockwise

rotation throughout the ejection phase. At AVC the mean LV rotation was 10.9 ± 4.8°. There was no global rotation of the RV until 50% of ejection time. From that time until AVC there was a minor clockwise rotation with maximum 1.4 ± 4.4°. A significant difference in global rotation was found in the time interval 50% ejection to AVC ($p < 0.05$).

Segmental analysis

The RV and the LV were divided in segments numbered according to figure 15, where the segments of the RV correspond to the segments of the LV. At the apical level of the LV all segments displayed a homogenous rotation during all of systole. The apical circumferential motion of the RV was less pronounced and heterogeneous throughout systole. The inferior and inferomedial segments (segment 3 and 4) of the RV rotated counter clockwise while the rest of the segments rotated clockwise (figure 16). Most prominent circumferential movement was seen in the anterior and anteroseptal segments (segment 1 and 6). Simultaneous opposite rotational directions between the anterior and the inferior segments (segment 1 and 4) of the RV was found in 10 out of 12 subjects. At the time of AVC there were significant differences in rotation between all corresponding segments (LV s1 vs RV s1. LV s2 vs RV s2 etc) of the two ventricles ($p < 0.05$) (table 2).

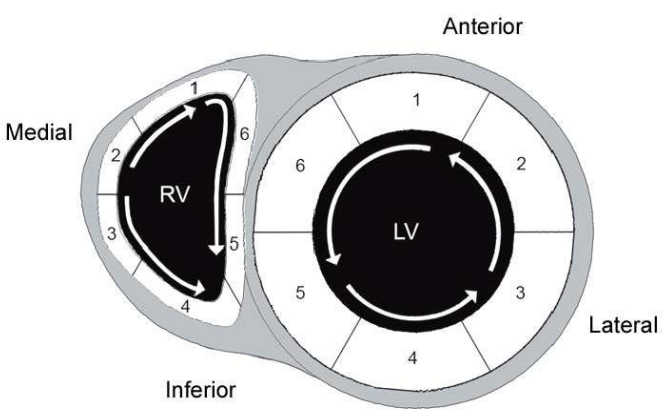

Figure 15. Location of the segments at both the left and the right ventricles within the ROI (segment 1-6). Corresponding segments of the LV and the RV are given the same numbers. Arrows indicate the circumferential motion during ejection.

Table 2. Degrees of rotation in each segment of both the left and the right ventricles at the time of aortic valve closure.

Segment	LV	RV	P
1	10.2±4.8	-4.5±4.5	0.01
2	11.2±4.7	-3.3±5.1	0.05
3	11.9±4.9	1.7±5.4	0.01
4	11.1±5.3	3.8±5.9	0.03
5	10.5±5.2	-0.4±4.4	0.01
6	10.4±4.8	-4.3±4.9	0.01

Positive values indicate counter-clockwise rotation and negative values indicate clockwise rotation. Mean ± standard deviation. P value <0.05 represents a significant difference in rotation between corresponding segments in the two ventricles. Segmental numbers according to figure 15.

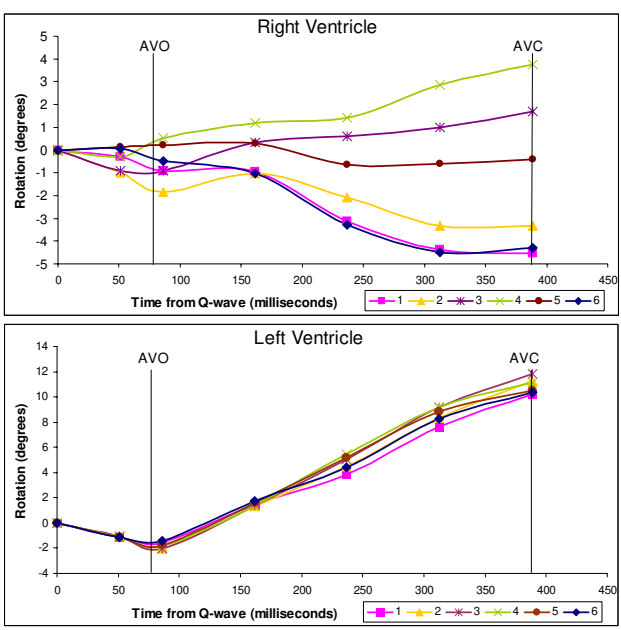

Figure 16. Regional rotation of the segments of the left and the right ventricles. The left ventricle have a uniform rotation. The right ventricle displays a heterogeneous rotation. AVO = aortic valve opening. AVC = aortic valve closure. Segmental numbers according to figure 15.

The rotation axis

Method

The method was developed to assess the orientation of the rotation axis of the LV at various levels. By measuring the geometry and regional rotation of the LV at three levels, basal mid and apical, simplified models of individual ventricles were created. By linear interpolation between the measured values of rotation the model was densely covered with coordinates of rotational information, making the method sensitive to even minor changes in regional rotation. To describe the orientation of the rotation axis, both degrees of deflection and direction are presented, either separately or as weighted mean. The deflection describes the angle ($angle_z$, °) between the rotation axis and the longitudinal axis of the LV. The direction ($angle_{xy}$, °) describes in what direction (0 - 360°) the axis is deflected, starting with zero degrees at the lateral segment and with increasing degrees counter clockwise. Weighted mean is based on a combination of deflection and direction.

The rotation axis in healthy humans

During the pre-ejection period the rotation axis displayed a significant and specific mean direction towards the anterolateral wall at the basal level ($p < 0.05$) (table 3 in supplements). At both basal and mid levels there was a significant and specific mean direction of the rotation axis towards mainly the inferior segments in the time interval 50% ejection to A-onset ($p < 0.01$). At the apical level there was a significant mean direction of the rotation axis towards the anteroseptal segments and gradually moving towards the septal segment in the time interval 75% ejection to A-onset ($p < 0.05$). The direction of the rotation axes are displayed individually in figure 17 and as weighted mean in figure 18. The deflection of the rotation axis always differed from the longitudinal axis of the LV in all tested time points.

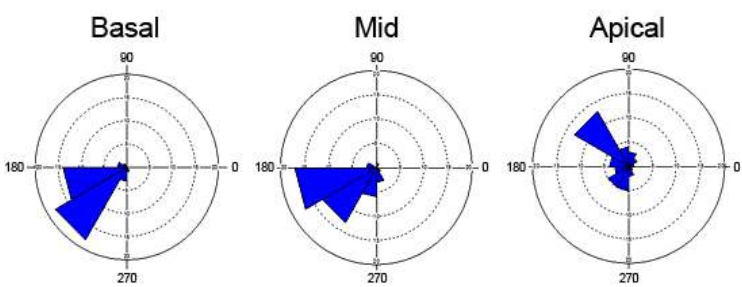

Figure 17. Histograms of the direction of the rotation axis at end of systole at different levels of the left ventricle in 39 healthy humans. Each circle within each graph represents 5 subjects. 0° = lateral, 90° = anterior, 180° = septal, 270° = inferior.

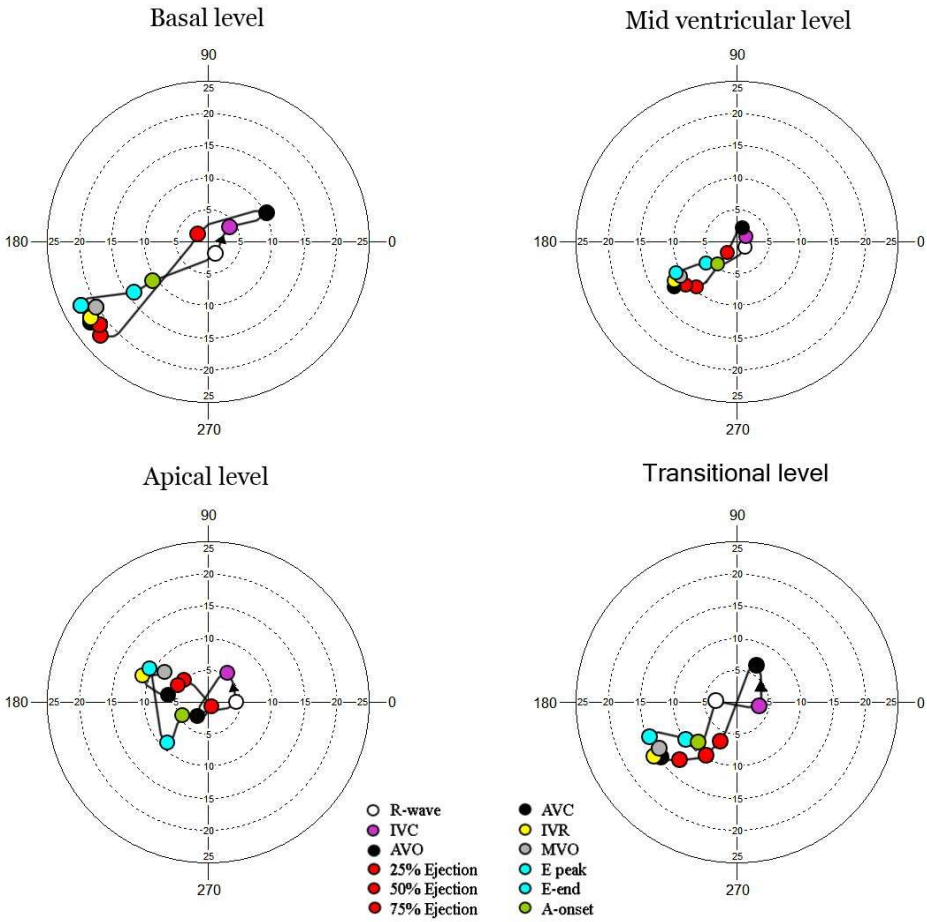

Figure 18. Weighted mean of deflection (angle$_z$, °) and direction (angle$_{xy}$, °) of the calculated rotation axes in 39 healthy subjects. Deflection is represented by the axial scale in the plots, and direction is represented by the circular scale in the plots and presented for discrete time points throughout the cardiac cycle at basal, mid, apical and transition levels. Every discrete point has been color-coded as defined at bottom. Ant, anteroseptal; ant, anterior; lat, lateral; post, posterior; inf, inferior; sept, septal. IVC, mid isovolumic contraction; AVO, aortic valve opening; AVC, aortic valve closure; IVR, mid isovolumic relaxation; MVO, mitral valve opening; E-peak, peak of early diastolic filling; E-end, end of early diastolic filling; A-onset, start of atrial wave.

The transition plane

A transition plane of the LV was present at almost all time points. Any absence of the transition plane was usually found in early systole when the direction of rotation changed at basal and apical levels. During most of the cardiac cycle the transition plane was located at 60-69% of the distance between apex and the basal level (z-level) (figure 19 a and table 4 in

supplements). The z-level of the transition plane was most stable at end of systole, where also least spread was seen. A correlation between the z-level of the transition plane and LV twist-ratio using cubic regression (r = 0.86), was found (figure 19 b). The direction of the normal axis to the transition plane over time resembles that of both the mid and basal levels, being directed towards the inferior segment during most of the cardiac cycle. The deflection of the normal axis to the transition plane was larger than at the mid level and less than at the basal level. This coincides with the transition plane being located between the basal level and the mid-level.

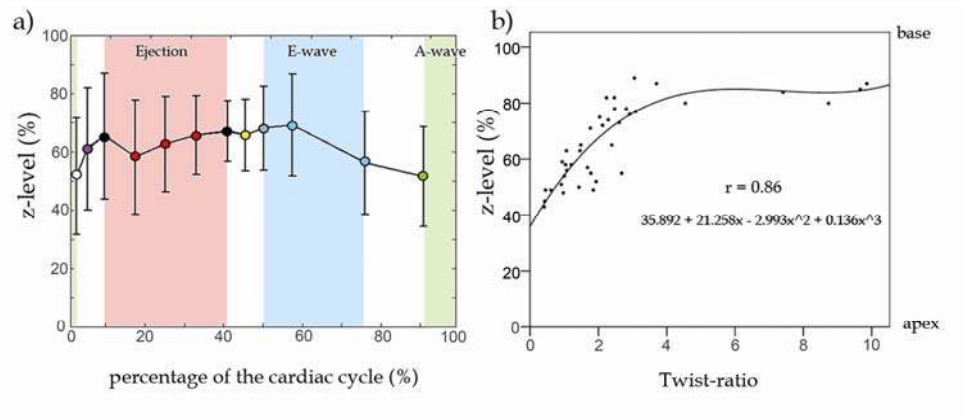

Figure 19. a) The z-level of the transition plane as a function of time. The mean z-level in percent (apex = 0% and basal level = 100%) measured for 12 time points in 39 healthy individuals are presented by the circular dots in the plot, whereas the standard deviations (± SD) are represented by the bars. The dots are colour-coded in the same way as in Figure 1, i.e. from left to right: R-wave, mid isovolumic contraction (IVC), aortic valve opening (AVO), 25%/50%/75% ejection, aortic valve closure (AVC), mid isovolumic relaxation (IVR), mitral valve opening (MVO), peak of early diastolic wave (E), end of E, onset of Atrial-wave. b) The relationship between the z-level of the transition plane and the left ventricular twist-ratio (apical rotation/-basal rotation) in 20 healthy subjects at two time points, one at time of mid ejection and one at end of systole.

Example of the rotation axis in a patient with reduced LV function.

The rotation pattern of the LV, as described by the deflection and the direction of the rotation axes, in the patient differed clearly from healthy subjects, as seen in figure 20. The direction of the rotation axis was towards the posterolateral wall during systole and most of diastole. In diastole there was an unstable rotation pattern, seen as movement of the rotation axis, compared to the stable untwist in healthy subjects. The transition plane was absent during most of the cardiac cycle, except during pre-ejection and at 50% and 75% of ejection time, indicating that there was no functional twist with opposite directions of rotation at the base and the apex.

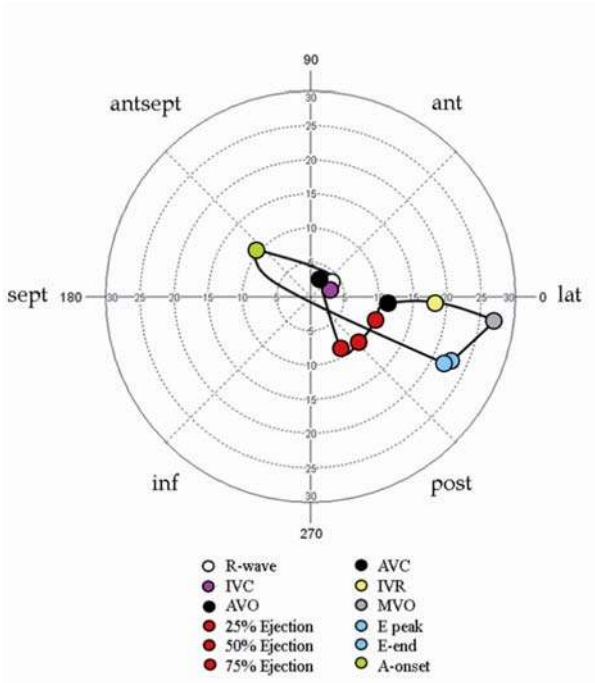

Figure 20. Mean direction (circular, °) and deflection (axial, °) of the rotation axis at mid ventricular level throughout the cardiac cycle in a patient with dilated cardiomyopathy and ejection fraction less than 30%, with most reduced function anteroseptally. Ant, anteroseptal; ant, anterior; lat, lateral; post, posterior; inf, inferior; sept, septal; IVC, mid isovolumic contraction; AVO, aortic valve opening; AVC, aortic valve closure; IVR, mid isovolumic relaxation; MVO, mitral valve opening; E-peak, peak of early diastolic filling; E-end, end of early diastolic filling; A-onset, start of atrial wave.

The rotation axis in acute ischemia

Rotation axis at baseline

At baseline there was little variation of the rotation axis during ejection and early diastole at mid and basal levels and the rotation axis was mainly directed towards the inferior wall (figure 21). At the apical level the rotation axis was mainly directed towards the anterior/anteroseptal wall, though with larger variations. There was a significant specific mean direction of the rotation axis present in the interval from AVO to MVO+50 ms at the basal level, between 50% ejection and MVO+50 ms at mid level and at R-wave and MVO+100 ms at the apical level. During the time interval between AVO and MVO+100 ms, the rotation axis had a mean deflection of 20.1 ± 5.8° at the basal level, 7.7 ± 3.6° at mid level and 5.6 ± 2.8° at the apical level.

Rotation axis during ischemia

At the basal level after 4 minutes of LAD occlusion the rotation axis was mainly directed towards the anterolateral wall with a mean deflection of 3.0 ± 1.4° during the time interval between AVO and MVO+100 ms (figure 21). A significant difference in direction of the rotation axis between baseline and after LAD occlusion was found in the interval between AVO to mid IVR and at MVO+100 ms at the basal level (table 5 in supplements). The deflection of the rotation axis had also significantly changed in the interval between 50% ejection to MVO+50 ms at the basal level and was 3.0 ± 1.4° ($p < 0.05$). At mid level the direction of the rotation axis had significantly changed at all but two time points (R-wave and AVO), being directed towards the anterior/anteroseptal wall. After LAD occlusion the mean deflection of the rotation axis at mid level was 6.5 ± 2.9° in the interval between AVO to MVO+100 ms. No significant difference in mean deflection of the rotation axis at mid level was found. At the apical level after LAD occlusion the rotation axis was still mainly directed towards the anterior/anteroseptal wall, however with a mean deflection of 9.7 ± 3.5°. There was a significant difference in both deflection and direction of the rotation axis at 25% ejection at the apical level.

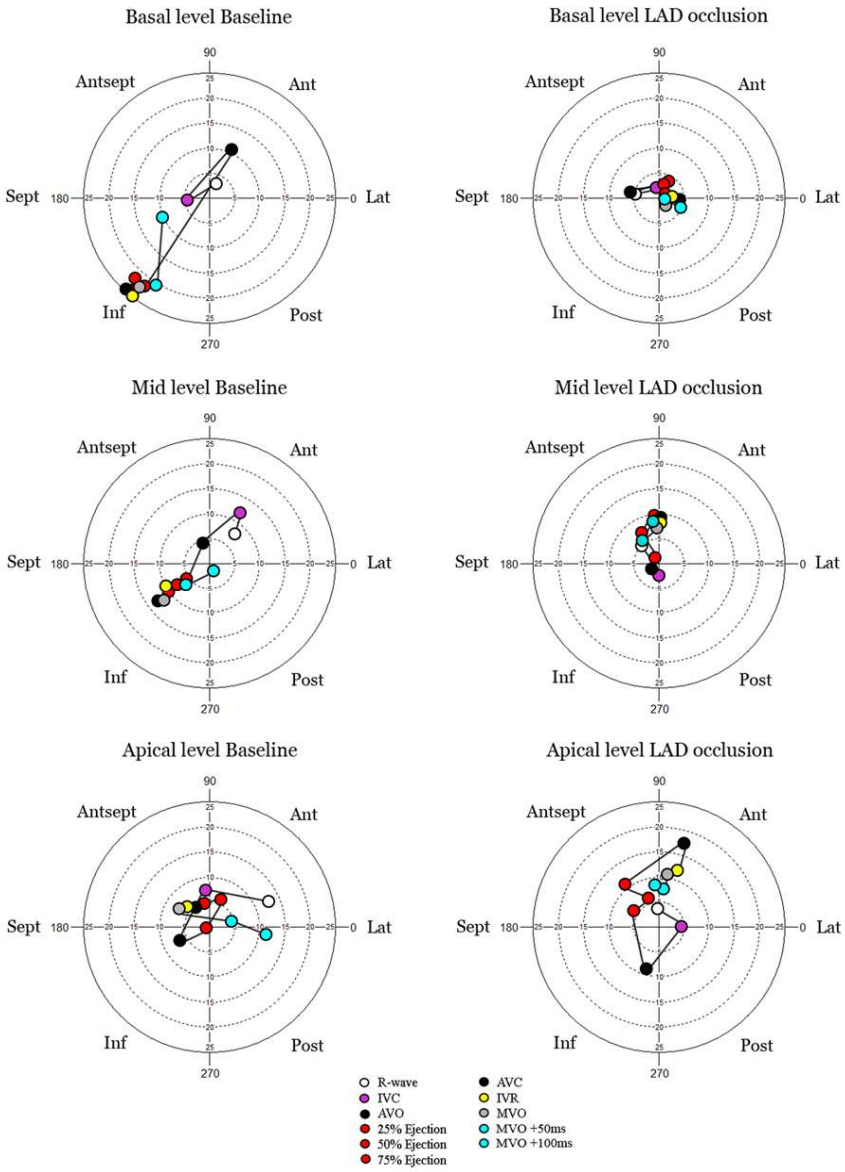

Figure 21. Each graph presents the weighted mean of the direction and deflection of the rotation axis at specific time points in the cardiac cycle in 6 pigs. The deflection is presented on the axial scale (°) and the direction on the circular scale (0-360°). The measured time points have been colour-coded according to bottom figure. Antsept = anteroseptal, Ant = anterior, Lat = lateral, Post = posterior, Inf = inferior, Sept = septal, IVC/R = mid isovolumic contraction, AVO/AVC = aortic valve opening/closure, IVR = mid isovolumic relaxation, MVO = mitral valve opening.

Stability of the rotation axis

There was a significant difference in stability of the rotation axis between baseline and after LAD occlusion at the basal level, (4.0 ± 5.2° vs 22.2 ± 24.7° respectively, $p < 0.05$). At mid level there was no significant difference in stability of the rotation axis. At the apical level there was a significant difference in stability of the rotation axis between baseline and after LAD occlusion (8.3 ± 8.8° and 30.5 ± 35.8° respectively, $p < 0.05$).

Rotation and twist

The basal rotation at AVC was 1.5 ± 2.9° and 1.2 ± 3.5° and the apical rotation at AVC was 10.6 ± 4.1° and 6.0 ± 4.9° at baseline and after LAD occlusion, respectively. There was no significant difference in rotation or twist amplitudes at any time point between baseline and during ischemia, neither in time to peak basal and apical rotation or twist.

AV-plane displacement

Results of AV-plane displacement are based on 5 pigs, as it could not be measured in one pig due to low image quality. A significant difference in septal AV-plane displacement between baseline and after 4 minutes of LAD occlusion was found (8.3 ± 1.5 mm to 6.2 ± 1.4 mm respectively, $p < 0.04$). A tendency of reduced AV-plane displacement in the lateral wall was also seen between baseline and after LAD occlusion (10.3±2.8 mm to 9.4±2.0 mm respectively, $p = 0.07$).

Wall motion score

Significantly reduced regional function by wall motion score was found in most areas generally supplied by LAD after occlusion of LAD (table 6). The number of affected segments at each level gradually increased towards the apex. The anterior segment had most reduced function at each level after LAD occlusion.

Table 6. Segmental wall motion score.

	Anteroseptal	Anterior	Lateral	Posterior	Inferior	Septal
Basal	1.0 / 2.5 *	1.0 / 2.5 *	1.0 / 1.8	1.0 / 1.0	1.0 / 1.0	1.0 / 1.5
Mid	1.3 / 2.8 *	1.3 / 2.8 *	1.2 / 1.8	1.0 / 1.0	1.0 / 1.0	1.0 / 2.2 *
Apical	1.8 / 2.8	1.5 / 2.8 *	1.2 / 2.3	1.0 / 1.2	1.0 / 1.8 *	1.5 / 2.7

Mean wall motion score (WMS) in 6 pigs at baseline / after4 minutes of LAD occlusion in 6 segments at three levels. The WMS scale is from 1 to 3, where 1 represents normal function and 3 akinesia. * indicates statistical significant difference of $p < 0.05$ between baseline and after LAD occlusion.

Reproducibility and quality measures

Rotation

The inter-observer variability had a CV of 0.4% when measuring in 5 subjects and an intra-observer CV of 5.0% when re-analyzing 15 subjects using the same ROI. Re-analyzing rotation using a new ROI in 6 subjects resulted in a CV of 18.5% at the basal level and 13.8% at the apical level.

Rotation axis

Within a rotation plane the mean deviation of the 6 rotation values, one from each segment, throughout the cardiac cycle (totally 667 frames) was 0.62 ± 0.43° at the basal level, 0.53 ± 0.34° at the mid level and 0.35 ± 0.31° at the apical level. Rotation planes could not be calculated in 0.6% of the frames at the basal level, 1.3% at the mid level and 1.8% at the apical level. When comparing the direction of the rotation axis of two different rotation analyses on each of the 10 subjects the correlation was $r = 0.91$ for all three levels and the deflection of the rotation axis had a CV of 14.8% at the basal level, 18.0% at mid level, 46.1% at the apical level and 18.9 at the transition level. The visually estimated and the calculated directions of the rotation axis were almost identical ($r = 0.99$) (figure 22). Between the estimated and calculated degrees of deflection there was a CV of 11.8% at the basal level, 20.6% at mid level, 15.8% at the apical level and 14.6% at the transition level. The CV of the Z-level between the estimated and calculated z-level of the transition plane was 5.1% and between the repeated rotation analyses 4.4%.

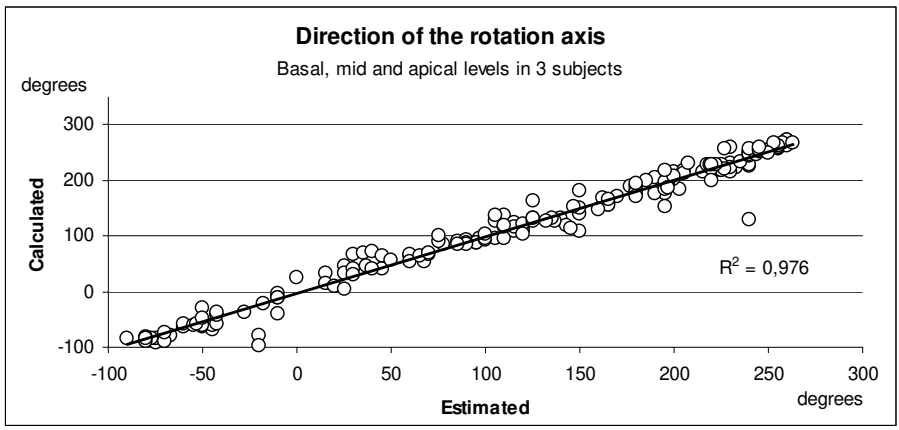

Figure 22. Typical example of the correlation of the estimated and the calculated directions of the rotation axis at basal, mid and apical levels in 3 randomly selected healthy subjects. Data is based on a circular scale between -90 and 270 degrees.

Discussion

These studies describe the rotation pattern of the LV and the apical circumferential motion of the RV in detail. By development of a new method to assess the axis around which the LV rotates, we introduce a new concept in cardiac function, the rotation axis. Study I and II describe the rotation pattern of the LV and the apical circumferential motion of the RV. Study III and IV describes the new method of the rotation axis and the effect of regional ischemia on the rotation pattern. The main finding of study I was the heterogeneity of rotation at basal and papillary levels, while the apical level displayed a homogenous rotation. Study II indicated that there is no functional apical rotation of the RV and that the circumferential motion at the RV apical level shortens towards the inferoseptal region, inducing a "belt action". Study III described the new method to calculate the rotation axis of the LV, based on regional differences in rotation within the LV, where a physiological pattern of the rotation axis was seen in healthy humans. Finally in study IV, the effect of acute ischemia on the rotation axis in pigs was studied. The rotation axis method was more sensitive than traditional parameters of rotation and at least as sensitive as AV-plane displacement measurements in detecting ischemia.

Left ventricular rotation

The importance of LV rotation and twist in ventricular function has become evident [46-49]. However, all implications of this twisting motion are not fully understood, as far as fundamental physiology of cardiac function. The twisting motion of the LV is considered to be the result of the contraction of the helical fibres of the LV [15, 16, 19]. The subepicardial fibres dominate the overall rotational motion due to the longer distance from the centre of the LV and more myocardial mass than the subepicardial portion [16, 50]. The contraction of the subepicardial fibres likely strengthens the outer shape of the LV, directing the myocardial thickening towards the centre of the LV and thus reducing the energy expenditure, which also has been suggested in a study by Bayar et al [51]. The differences in regional rotation, with most clockwise rotation in the inferoseptal regions and least clockwise rotation in the anterolateral regions at mid and basal levels of the LV might be explained by the anatomy and the activation sequence of the LV. Greenbaum et al showed that the anterolateral wall have less obliquely orientated fibres than other walls of the LV [15]. This supports our finding of regional differences in rotation, and other studies have confirmed the heterogenous rotation of the LV [52, 53]. The activation pattern of the LV is probably also of

importance to the rotational motion of the LV. The septum being activated first, followed by the endocardium and later the epicardium, activated from apex to base, generates temporal differences in apical and basal rotation and might augment the regional differences seen [54, 55]. The early systolic untwist, both seen at basal and apical levels, is likely the effect of the early activation of the subendocardium and the right handed helix. Our findings also displayed a temporal difference in early systolic untwist between the apical and the basal levels. The apical untwist, starting after the electrical activation of the LV and ending at AVO, indicates to be an active and well synchronized motion. The basal untwist started concurrently with the atrial contraction and continued well into the ejection phase, indicating a passive onset and a prolonged and less synchronized motion compared to the apical early systolic untwist. As LV twist is associated with increase of ventricular pressure and untwist with decrease of pressure, this sequence of systolic rotation is likely of importance for optimal ventricular function [56-58]. Studies have suggested that the temporal differences in the activation pattern contribute in directing the blood towards the outflow tract in early systole [59, 60]. The earlier onset of systolic rotation at the apex compared to the base would create an intraventricular pressure gradient, driving blood towards the base. An experimental study in dogs indicated an early systolic pressure difference between the base and the apex, supporting this theory [61]. Even though there seems to be a temporal difference in onset of systolic rotation, both basal and apical systolic rotations end more synchronized close to the time of AVC. The synchronized offset of systolic rotation and onset of untwist of the LV probably plays an important role in the rapid reduction of ventricular pressure, augmenting ventricular filling, as have been indicated by other studies [46, 47, 58, 62].

The well-timed onset of basal and apical untwist is followed by temporal differences in duration of rotation. Untwist at the basal level occurred in two phases, while untwist at the apical level only occurred in one phase. The early untwist at the basal level ended at peak mitral filling (peak E), while apical untwist continued throughout the early filling phase. This difference probably aids in creating intraventricular pressure differences, distributing blood from the basal to the apical part to optimize ventricular filling, not just only during the active filling but also during IVR. Studies have shown that during IVR there is a rapid base-to-apex reversal of blood flow, supporting this theory [59, 63]. During the late filling (A-wave) there was a minor untwist of the basal level which continued into early systole, while almost no apical untwist occurred. This probably reverses the pressure difference between apex and base, reducing the motion of blood towards the apex. Studies have shown that there are intraventricular pressure differences at both early diastole and late diastole, which support the theories mentioned above [58, 61].

This, combined with studies describing the importance of rotation in systolic function, indicates that rotation plays an important role in both systolic and diastolic ventricular function [46, 64-66].

Right ventricular apical circumferential motion

The study of the circumferential apical motion of the RV, by using STE was the first published of its kind. RV function has previously been underestimated as LV function was much considered as the central part of cardiac function [67]. However, studies have now demonstrated the importance of the RV in cardiac function and survival [68-71]. The longitudinal and radial motions of the RV are the main contributors to RV function [30, 31]. The myocardial fibre orientation of the RV, with predominantly longitudinally and circumferentially orientated fibres, differs from that of the LV, where additionally obliquely or helically fibres exist to a large extent [15]. The lack of obliquely orientated fibres in the RV could be an adaptation to the relatively low pressure environment in which it performs. No additional stabilising structure, in form of helical fibres, might be needed to optimize RV function and would only increase the energy consumption. The shape of the RV, being far from circular in short axis view, also differs from the LV. The ventricles have about the same volumes, but the endocardial area of the RV is greater than that of the LV, due to the difference in shape of the ventricles. This results in less required radial shortening of the RV to produce equal stroke volume to the LV [13]. The environment, shape and anatomy of the RV indicate that it is not constructed for creating a rotational motion, which support our finding of a non-functional rotation of the RV apex.

The circumferential shortening at the RV apical level is primarily constituted by the free wall moving towards the septum, which is seen as a bidirectional rotation. Along with the rotational motion of the septum, mainly generated by the LV, the apical circumferential motion of the RV can be described as a "belt action" motion, where the anterior, septal and inferior parts all move towards the intersection between the inferior and septal segments. The apical part of the RV is sort of rolled up on the LV during systole and rolled back during diastole. This could be an efficient way of displacing the myocardium of the RV by using the rotation of the LV as a contributing force in reducing the RV volume. The "belt action" likely reduces interventricular stress, as the RV probably benefits of LV rotation in both systole and diastole. Studies have demonstrated the dependence of RV function on LV function which supports these findings [35-37].

The rotation axis

By development of this new method to assess the rotation axis of the LV, we introduce a new concept in ventricular function, the rotation axis. The commercial methods to assess LV rotation are based on measurements of rotation around the longitudinal axis of the LV. The combination of the general approach to measure rotation and the finding of opposite directions of rotation at the base and apex makes it is easy to assume that the LV rotates around its longitudinal axis. However, the axis the LV rotates around has never before been established, why such an assumption has no ground. The regional differences in rotation reported in healthy humans indicate that the LV is not designed to rotate around its longitudinal axis [52, 53]. Our findings clearly support the idea that the axis the LV rotates around is different from the longitudinal axis. The rotation axis of the LV is dynamic and displays a consistent physiological pattern in healthy subjects.

Method

The method of assessing the rotation axis is based on identifying levels or planes with similar rotation in the LV. This is derived from regional rotation amplitudes, where the relative relationship between rotation values is calculated. The result of the rotation axis method does not present the amplitude of rotation, in contrast to the commercial methods which only focus on the amplitude of rotation. The rotation axis method uniquely describes the rotation pattern or how the LV rotates, instead of how much it rotates. To further develop the method and possibly simplifying the visual overview, all rotation axes could be condensed into one rotation axis describing all rotation axes of the LV, called the torsion axis. The torsion axis would be a curved rotation axis presented in 3D, reflecting the rotation axis at any level, see figure 23.

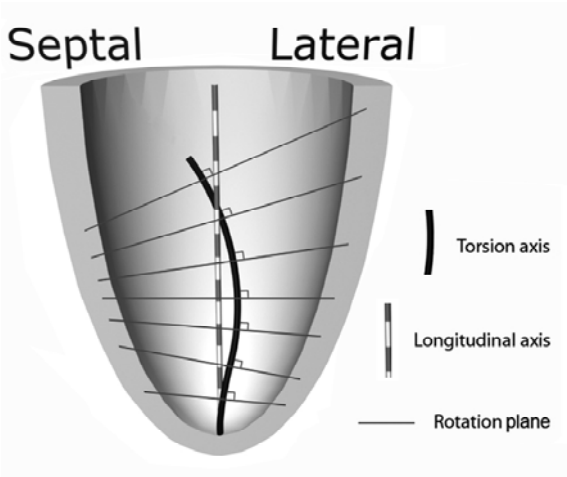

Figure 23. The left ventricle and the mean torsion axis of 39 healthy subjects at end systole. The torsion axis is perpendicular to the rotation plane at any specific level.

Rotation axis in healthy humans

The motion of the rotation axes seem linked to different phases of the cardiac cycle. The early systolic event, with untwist of the ventricle, was indicated at all levels by the mean rotation axes being orientated in a different direction than during the ejection phase. There could also be a temporal dispersion from apex to base in the change from the early systolic event to the main systolic event of the rotation axes, which probably is associated with the activation pattern of the LV. During the main systolic event and early diastole the rotation axes remained fairly stationary, even though the twisting and untwisting motion is most pronounced during this period. This indicates a symmetrical rotational motion of the LV, both during contraction and relaxation. This means that the relationship in rotation between different segments is uniform. It also displays the methods independence of rotation or twist amplitudes. During the second half of the early filling phase there was a change in orientation of the rotation axes at all levels, as they started to move closer to the inflow area. Even the diastasis was indicated, primarily at basal and mid levels, by the rotation axes being fairly stationary during this period. The physiological pattern displayed by the rotation axis, associated to anatomy, activation pattern and regional myocardial function, adds information on LV function and has likely the potential to identify LV pathologies, as indicated by the results of the patient with reduced LV function. The reproducibility, quality measurements and results of the rotation axis, showing little variation in late systole and early diastole, support the possibility that the method could be used to differentiate between health and disease.

Transition plane

There are a few studies that have discussed the transition level or equatorial level of the LV [72, 73]. However, none have previously calculated either position or the angle of the transition plane. The transition between basal and apical rotation was successfully identified by our new method and its dynamic motion could be calculated throughout the cardiac cycle. The occurrence of a transition plane is an indication of opposite rotational directions at the basal and apical levels. The stable position of the transition plane at about mid or upper part of the papillary muscles during most of systole and early diastole, seen in healthy humans, indicate that the position could be of importance for the function of the papillary muscles. As the transition plane is located at the papillary muscles there is only minor circumferential displacement of the papillary muscles. This could aid in the function of the mitral valve, by maintaining the position of the papillary muscles in reference to the mitral valve. As the position of the transition plane seems strongly associated with the ratio between basal and apical rotation, it is likely that patients with reduced apical rotation have their transition plane displaced closer to the apex. It has been suggested that ventricular hypertrophy and apical function could determine the z-level of the transition plane which is in accordance with our findings [72]. The occurrence and position of the transition plane could itself be a marker of ventricular function.

Rotation and the rotation axis in acute ischemia

There is more to rotational function of the LV than amplitudes and timings. The rotation pattern needs to be considered as well. Study IV indicates that the acute effect of ischemia mainly affects the rotation pattern of the LV and to a lesser extent amplitudes or timings of rotation. The experimental study on pigs confirms the finding in humans that the LV does not rotate around its longitudinal axis in normal conditions.

As shown by Helle-Valle et al and Bansal et al, regional rotation has limited ability in detecting areas of reduced function [74, 75]. However, in a study by Sun et al, inducing LAD occlusion in pigs, they observed significantly reduced torsion in the anterior segment but no globally reduced torsion [76]. Bansal et al also showed that global rotation was most dependent on the size of myocardial infarction rather than the location of the infarction. Additionally, they observed that the basal rotation was more reduced than the apical rotation in patients with infarction, explained by the fact that the apex is less attached to other structures and is more prone to maintain its motion. This theory does not support our findings that rotation was

primarily reduced at the apical level, though non-significantly, in ventricles with reduced function. Other studies confirm our findings that the apical level seems more sensitive to changes in LV function than the basal level [77, 78]. The combination of limited ability to detect regional dysfunction and the wide range of amplitudes reported in healthy humans indicate that measuring rotation amplitudes has clear limitations as a marker for dysfunction for individuals [79, 80]. The fact that global rotation seems relatively unaffected by regional dysfunction and studies demonstrating rotation to be preserved or even increased in some pathological states could support the idea that there is a rotational reserve acting as a compensating force to maintain adequate cardiac output [81-83]. If so, this could in part explain why amplitudes of rotation seem less sensitive in identifying regional changes in function.

Within the ischemic area it would be likely to have reduced function in all the involved myocardial fibres. After 4 minutes of LAD occlusion the ischemia is probably transmural in most of the affected area. Therefore it would be likely to assume the helical fibres to be equally affected as the circumferential and longitudinal fibres. However, despite the obvious differences in regional function after occluding LAD, no significant differences in rotation amplitudes or timings could be detected. Both AV-plane displacement and WMS showed significant changes, though non-specific and by subjective assessment, respectively. Occluding LAD in humans reduces the longitudinal function in not just the septal wall but also in the lateral wall, as shown by Henein et al, suggesting AV-plane displacement being sensitive but non-specific to regional ischemia [84]. The objective rotation axis differed significantly after LAD occlusion and displayed a fairly consistent pattern both before and after LAD occlusion. This indicates that rotation is as sensitive to regional ischemia as longitudinal and radial functions of the LV. It is just a matter of finding the right tool to demonstrate it. This is further supported by the results of WMS and the direction of the rotation axes, which indicated a relationship between the rotation pattern and regional myocardial function. The response to regional dysfunction suggests that the rotation axis could be a marker for ventricular function and could have potential for indicating dysfunctional areas.

By observing the motion of the rotation axes over time, symmetry in the rotation pattern can be assessed. In normal conditions in humans and at baseline in the experimental animal study the rotation axes displayed a stationary position at late systole and early diastole. After inducing ischemia the rotation pattern became less stable, at both basal and apical levels, indicating myocardial incoordination. Another indication of dysfunctional

rotation is the change in deflection of the rotation axes. At the basal level the deflection was reduced while increased at the apical level after LAD occlusion, indicating reduced regional differences in rotation at the base and increased differences at the apex. The aspect of studying rotational symmetry in this way provides both a global and regional view of myocardial coordination, which is unique. This could be an alternative approach to measuring ventricular dyssynchrony and could aid in selecting patients for cardiac resynchronization therapy (CRT) or optimization of the CRT device.

Limitations

Left and right ventricular rotation

Time measurements of cardiac events were made in separate cardiac cycles and applied to other cardiac cycles with similar heart rate. The setting of the ROI in rotation analyses affects the result and even minor changes of the ROI changes the peak rotation amplitudes by up to 19%. Due to technical difficulties in acquiring sufficient signal quality in simultaneous recordings of both left and right ventricles at the apical levels, more than half of the study population was excluded. The speckle tracking software made placement of the ROI difficult in the transition between the free wall of the RV and the septum.

Rotation axis

Construction of an individual, dynamic 3D model of the LV based on 2D measurements is a simplification of reality. Furthermore, the model is based on assumptions of a linear relationship between rotation at different levels of the LV and also linear geometrical changes over time within systole and diastole. However, despite these limitations, the method still seems sensitive to changes in regional rotation. The differences in deflection of the rotation axis seen when testing the reproducibility in re-analyzed rotation analyses depend most likely in differences between the speckle tracking analyses. Compared to the manual estimations of deflection, the difference in deflection was less pronounced, which support our interpretation that the calculations of the rotation axis probably are accurate. The rotation axis cannot be calculated in frames where there are larger differences than 0.5° of rotation between opposite sides of the LV. To increase the accuracy of geometric measurements over time, 3D echocardiography could be used and with the advance in 3D speckle tracking regional rotation could perhaps also be more accurately described.

The effect of negative inotropic drugs on the results of the calculations of the rotation axis is unclear. However, as it reduces cardiac function it could have reduced the relative differences between baseline and after LAD occlusion, making it more difficult to retain significant differences. The occlusion of LAD could have varied between the pigs, inducing a proximal or mid LAD occlusion. The size of the ischemic area was not determined by any method, other than by indication of the result of WMS.

Main Findings

Study I. There were large regional differences in regional rotation in healthy subjects, both between the base and the apex and within basal and mid ventricular levels. Diastolic untwist matches the filling phases E and A, underlining the important role in filling. Early untwist at the apex, related to E and LV suction, likely actively facilitates early apical filling. Late untwist at basal level seems passive, generated by atrial contraction.

Study II. There was a clear difference in rotational function of the two ventricles, probably based on the underlying myocardial fibre structure. LV apical systolic rotation was counter clockwise in all segments while the RV segments were brought together toward the inferoseptal region, inducing a ´tightening belt´ mechanism for reducing its cavity circumference. The prominent LV apical rotation could contribute to the suggested mechanism.

Study III. We introduce a new concept to evaluate LV function, achieved by development of a novel method to calculate the rotation axis of the LV. This method provides a unique overview of the rotation pattern of the LV throughout the cardiac cycle. The axis of rotation at different levels of the LV displayed a physiological pattern, where also stability of the rotation pattern could be assessed. Furthermore, the angle and level of the transition plane could be described over time. This new way of assessing rotational function provides further insight into the complexity of LV mechanics. The method has acceptable reproducibility and the potential clinical use of this method will be validated in further studies.

Study IV. Regional myocardial ischemia, by LAD occlusion, changes the rotation pattern of the LV dramatically. The new method of assessing the rotation axis seems superior in detecting regional dysfunction than measurements of rotation and twist amplitudes and as sensitive as AV-plane displacement. Additionally, the rotation axis method could assess myocardial incoordination and could have the potential to localise areas with disturbed myocardial function.

Conclusion

Rotation plays an important role in LV function, as rotation is strongly associated with ejection and filling. In difference to the LV, the RV did not show any functional rotation. However, its heterogeneous circumferential motion could still be of importance to RV function and may in part be the result of ventricular interaction. The myocardial structure of the LV, creating the twisting motion with regional differences, is probably designed to optimize ventricular function with minimal energy expenditure. The time sequence of regional rotation of the LV aids in intra-ventricular blood distribution in early diastole and most likely in early systole to optimize filling end ejection. These associations are based on studies of mean amplitudes of rotation at basal and apical levels. However, LV rotation is more complex than regional amplitudes and timings. Other aspects of the rotation pattern also need to be considered to fully understand the function and importance of the rotational motion. By analysing the rotation axis of the LV, a new aspect of the rotation pattern can now be visualized and quantified. The rotation axis, based on calculations of planes with equal rotation, provides a unique overview of the rotation pattern of the LV. As the rotation pattern is the result of regional contractility and timing of activation, the results of this new method could have the potential for assessing regional function and mechanical synchrony. Preliminary results based on this new approach indicate that changes in rotational function could easier be detected than by conventional methods of measuring the rotational function of the LV. Potential future implications of this new method could be in early detection of cardiac dysfunction, assessing mechanical dyssynchrony and optimization of CRT. However, two of the remaining challenges in this new approach are to further evolve the interpretation of the results and finally to create clinical relevant reference values.

Acknowledgements

To all of you who have helped me during this time, all from co-authors to people who just lightens my day, thank you all.

First of all, I would like to express my deepest gratitude to my head supervisor and friend **Anders Waldenström**. Your encouragement, support, believes in me and great knowledge in cardiology has helped me through these years.

Per Lindqvist, for keeping me on track and always trying to make me see the big picture, and also for being a friend. **Stellan Mörner**, for support, intellectual conversations and comments and for the help with the papers and abstracts. **Matilda Larsson** and **Anna Bjällmark**, for your clever solutions to all problems encountered when developing the method and for always having a smile on your faces.

Michael Haney, for your great knowledge in animal research, always being positive and your scientific contributions in paper IV and my thesis. Looking forward towards future collaborations. **Roman A´Roch**, for your help in the animal lab and your positive and enthusiastic research approach, which is a bit contagious. **Göran Johansson**, for all help with technical registrations in the animal lab. **Michael Henein**, for all interesting scientific conversations and always being positive and friendly. **Lars-Åke Brodin**, for always providing interesting ideas and being able to see physiology from a technical perspective and your positive attitude.

Kerstin Rosenqvist and **Eva Karlsson**, all your help with everything have kept me on track during theese years and thank you for being great lunch-dates. **Maria Backlund**, for practial assistance and being a good travel companion. **Caroline Mellberg**, for support and being a good friend and travel companion. **Elin Asplund**, for continuing my research, giving me inspiration and being positive and funny.

Christer Backman, for help with paper IV, great knowledge in physiology and echocardiography and for all you've taught me in echocardiography. **Eva Karlendal**, for your support and understanding during these years. To the **staff of clinical physiology**, thank you for being understanding and positive to my research.

Åsa, Anny and **Nelli,** for your support, being there for me and putting out with me during these years and for all joy you have brought into my life.

References

1. Ghalioungui P. The Ebers Papyrus. A new English translation, commentaries and glossaries.: Academy of Scientific Research and Technology, Cairo 1987.
2. Saba MM, Ventura HO, Saleh M, Mehra MR. Ancient Egyptian medicine and the concept of heart failure. Journal of cardiac failure 2006;12:416-21.
3. Da Vinci L. Starling's Principles of Human Physiology. London, UK: JA Churchill 1936;Quoted by Evans L:1.
4. Keele K. Leonardo da Vinci's Elements of the Science of Man New York, USA: Academic Press 1983.
5. Thiene G. The discovery of cirulation and the origin of modern medicine during the Italian Renaissance. Cardiol Young 1996;6:109-19.
6. Harvey W. An anatomical disquisition on the motion of the heart and blood in animals (1628). In: Willis FA, Keys TE, eds Cardiac classics London: Henry Kimpton, 1941: 19-79.
7. Lower R. Tractus de Corde. Oxford, UK: Dawsons, Pall Mall, London 1968.
8. Wiggers C. Studies on the consecutive phases of the cardiac cycle. The duration of the consecutive phases of the cardiac cycle and the criteria for their precise determination. Am J Physiol 1921:415-38.
9. Fukuta H, Little WC. The cardiac cycle and the physiologic basis of left ventricular contraction, ejection, relaxation, and filling. Heart failure clinics 2008;4:1-11.
10. Smalcelj A, Gibson DG. Relation between mitral valve closure and early systolic function of the left ventricle. British heart journal 1985;53:436-42.
11. von Bibra H, Wirtzfeld A, Hall R, Ulm K, Blomer H. Mitral valve closure and left ventricular filling time in patients with VDD pacemakers. Assessment of the onset of left ventricular systole and the end of diastole. British heart journal 1986;55:355-63.
12. Waider W, Craige E. First heart sound and ejection sounds. Echocardiographic and phonocardiographic correlation with valvular events. The American journal of cardiology 1975;35:346-56.
13. Rushmer R. Cardiovasular Dynamics. 3 ed: W. B. Saunders Company; 1970.
14. Sallin EA. Fiber orientation and ejection fraction in the human left ventricle. Biophysical journal 1969;9:954-64.
15. Greenbaum RA, Ho SY, Gibson DG, Becker AE, Anderson RH. Left ventricular fibre architecture in man. British heart journal 1981;45:248-63.

16. Lunkenheimer PP, Redmann K, Kling N, et al. Three-dimensional architecture of the left ventricular myocardium. Anat Rec A Discov Mol Cell Evol Biol 2006;288:565-78.
17. Streeter DD, Jr., Spotnitz HM, Patel DP, Ross J, Jr., Sonnenblick EH. Fiber orientation in the canine left ventricle during diastole and systole. Circ Res 1969;24:339-47.
18. Arts T, Meerbaum S, Reneman RS, Corday E. Torsion of the left ventricle during the ejection phase in the intact dog. Cardiovasc Res 1984;18:183-93.
19. Ingels NB, Jr., Hansen DE, Daughters GT, 2nd, Stinson EB, Alderman EL, Miller DC. Relation between longitudinal, circumferential, and oblique shortening and torsional deformation in the left ventricle of the transplanted human heart. Circ Res 1989;64:915-27.
20. Ingels NB, Jr. Myocardial fiber architecture and left ventricular function. Technol Health Care 1997;5:45-52.
21. Gibbons Kroeker CA, Ter Keurs HE, Knudtson ML, Tyberg JV, Beyar R. An optical device to measure the dynamics of apex rotation of the left ventricle. Am J Physiol 1993;265:H1444-9.
22. Sengupta PP, Korinek J, Belohlavek M, et al. Left ventricular structure and function: basic science for cardiac imaging. Journal of the American College of Cardiology 2006;48:1988-2001.
23. Gustafsson U, Lindqvist P, Morner S, Waldenstrom A. Assessment of regional rotation patterns improves the understanding of the systolic and diastolic left ventricular function: an echocardiographic speckle-tracking study in healthy individuals. Eur J Echocardiogr 2009;10:56-61.
24. Rosen BD, Gerber BL, Edvardsen T, et al. Late systolic onset of regional LV relaxation demonstrated in three-dimensional space by MRI tissue tagging. American journal of physiology 2004;287:H1740-6.
25. Guron CW, Hartford M, Persson A, Herlitz J, Thelle D, Caidahl K. Timing of regional left ventricular lengthening by pulsed tissue Doppler. J Am Soc Echocardiogr 2004;17:307-12.
26. Esch BT, Scott JM, Warburton DE, et al. Left ventricular torsion and untwisting during exercise in heart transplant recipients. The Journal of physiology 2009;587:2375-86.
27. Galiuto L, Ignone G, DeMaria AN. Contraction and relaxation velocities of the normal left ventricle using pulsed-wave tissue Doppler echocardiography. The American journal of cardiology 1998;81:609-14.
28. Greaves K, Puranik R, O'Leary JJ, Celermajer DS. Myocardial tissue velocities in the normal left and right ventricle: relationships and predictors. Heart, lung & circulation 2004;13:367-73.

29. Notomi Y, Popovic ZB, Yamada H, et al. Ventricular untwisting: a temporal link between left ventricular relaxation and suction. American journal of physiology 2008;294:H505-13.
30. Carlsson M, Ugander M, Heiberg E, Arheden H. The quantitative relationship between longitudinal and radial function in left, right, and total heart pumping in humans. American journal of physiology 2007;293:H636-44.
31. Haddad F, Hunt SA, Rosenthal DN, Murphy DJ. Right ventricular function in cardiovascular disease, part I: Anatomy, physiology, aging, and functional assessment of the right ventricle. Circulation 2008;117:1436-48.
32. Haber I, Metaxas DN, Geva T, Axel L. Three-dimensional systolic kinematics of the right ventricle. American journal of physiology 2005;289:H1826-33.
33. Klein SS, Graham TP, Jr., Lorenz CH. Noninvasive delineation of normal right ventricular contractile motion with magnetic resonance imaging myocardial tagging. Ann Biomed Eng 1998;26:756-63.
34. Pettersen E, Helle-Valle T, Edvardsen T, et al. Contraction pattern of the systemic right ventricle shift from longitudinal to circumferential shortening and absent global ventricular torsion. Journal of the American College of Cardiology 2007;49:2450-6.
35. Damiano RJ, Jr., La Follette P, Jr., Cox JL, Lowe JE, Santamore WP. Significant left ventricular contribution to right ventricular systolic function. Am J Physiol 1991;261:H1514-24.
36. Saleh S, Liakopoulos OJ, Buckberg GD. The septal motor of biventricular function. Eur J Cardiothorac Surg 2006;29 Suppl 1:S126-38.
37. Santamore WP, Dell'Italia LJ. Ventricular interdependence: significant left ventricular contributions to right ventricular systolic function. Prog Cardiovasc Dis 1998;40:289-308.
38. Notomi Y, Lysyansky P, Setser RM, et al. Measurement of ventricular torsion by two-dimensional ultrasound speckle tracking imaging. Journal of the American College of Cardiology 2005;45:2034-41.
39. Helle-Valle T, Crosby J, Edvardsen T, et al. New noninvasive method for assessment of left ventricular rotation: speckle tracking echocardiography. Circulation 2005;112:3149-56.
40. Amundsen BH, Helle-Valle T, Edvardsen T, et al. Noninvasive myocardial strain measurement by speckle tracking echocardiography: validation against sonomicrometry and tagged magnetic resonance imaging. Journal of the American College of Cardiology 2006;47:789-93.
41. A'Roch R, Steendijk P, Oldner A, et al. Left ventricular mechanical dyssynchrony is load independent at rest and during

endotoxaemia in a porcine model. Acta physiologica (Oxford, England) 2009;196:375-83.
42. Lang RM, Bierig M, Devereux RB, et al. Recommendations for chamber quantification: a report from the American Society of Echocardiography's Guidelines and Standards Committee and the Chamber Quantification Writing Group, developed in conjunction with the European Association of Echocardiography, a branch of the European Society of Cardiology. J Am Soc Echocardiogr 2005;18:1440-63.
43. Quinones MA, Otto CM, Stoddard M, Waggoner A, Zoghbi WA. Recommendations for quantification of Doppler echocardiography: a report from the Doppler Quantification Task Force of the Nomenclature and Standards Committee of the American Society of Echocardiography. J Am Soc Echocardiogr 2002;15:167-84.
44. Crick SJ, Sheppard MN, Ho SY, Gebstein L, Anderson RH. Anatomy of the pig heart: comparisons with normal human cardiac structure. Journal of anatomy 1998;193 (Pt 1):105-19.
45. Bland JM, Altman DG. Statistical methods for assessing agreement between two methods of clinical measurement. Lancet 1986;1:307-10.
46. Notomi Y, Martin-Miklovic MG, Oryszak SJ, et al. Enhanced ventricular untwisting during exercise: a mechanistic manifestation of elastic recoil described by Doppler tissue imaging. Circulation 2006;113:2524-33.
47. Rademakers FE, Buchalter MB, Rogers WJ, et al. Dissociation between left ventricular untwisting and filling. Accentuation by catecholamines. Circulation 1992;85:1572-81.
48. Tibayan FA, Rodriguez F, Langer F, et al. Alterations in left ventricular torsion and diastolic recoil after myocardial infarction with and without chronic ischemic mitral regurgitation. Circulation 2004;110:II109-14.
49. Dong SJ, Hees PS, Huang WM, Buffer SA, Jr., Weiss JL, Shapiro EP. Independent effects of preload, afterload, and contractility on left ventricular torsion. Am J Physiol 1999;277:H1053-60.
50. Burns AT, McDonald IG, Thomas JD, Macisaac A, Prior D. Doin' the twist: new tools for an old concept of myocardial function. Heart (British Cardiac Society) 2008;94:978-83.
51. Beyar R, Sideman S. Effect of the twisting motion on the nonuniformities of transmyocardial fiber mechanics and energy demand--a theoretical study. IEEE transactions on bio-medical engineering 1985;32:764-9.
52. Dong L, Zhang F, Shu X, Guan L, Chen H. Left ventricular torsion in patients with secundum atrial septal defect. Circ J 2009;73:1308-14.

53. van Dalen BM, Soliman OI, Vletter WB, ten Cate FJ, Geleijnse ML. Insights into left ventricular function from the time course of regional and global rotation by speckle tracking echocardiography. Echocardiography (Mount Kisco, NY 2009;26:371-7.
54. Kavanagh KM, Belenkie I, Duff HJ. Transmural temporospatial left ventricular activation during pacing from different sites: potential implications for optimal pacing. Cardiovascular research 2008;77:81-8.
55. Sengupta PP, Khandheria BK, Korinek J, Wang J, Belohlavek M. Biphasic tissue Doppler waveforms during isovolumic phases are associated with asynchronous deformation of subendocardial and subepicardial layers. J Appl Physiol 2005;99:1104-11.
56. Moon MR, Ingels NB, Jr., Daughters GT, 2nd, Stinson EB, Hansen DE, Miller DC. Alterations in left ventricular twist mechanics with inotropic stimulation and volume loading in human subjects. Circulation 1994;89:142-50.
57. Gibbons Kroeker CA, Tyberg JV, Beyar R. Effects of load manipulations, heart rate, and contractility on left ventricular apical rotation. An experimental study in anesthetized dogs. Circulation 1995;92:130-41.
58. Nikolic SD, Feneley MP, Pajaro OE, Rankin JS, Yellin EL. Origin of regional pressure gradients in the left ventricle during early diastole. Am J Physiol 1995;268:H550-7.
59. Sengupta PP, Khandheria BK, Korinek J, et al. Left ventricular isovolumic flow sequence during sinus and paced rhythms: new insights from use of high-resolution Doppler and ultrasonic digital particle imaging velocimetry. Journal of the American College of Cardiology 2007;49:899-908.
60. Sedmera D. Form follows function: developmental and physiological view on ventricular myocardial architecture. Eur J Cardiothorac Surg 2005;28:526-8.
61. Courtois M, Kovacs SJ, Jr., Ludbrook PA. Transmitral pressure-flow velocity relation. Importance of regional pressure gradients in the left ventricle during diastole. Circulation 1988;78:661-71.
62. Esch BT, Warburton DE. Left ventricular torsion and recoil: implications for exercise performance and cardiovascular disease. J Appl Physiol 2009;106:362-9.
63. Voon WC, Su HM, Yen HW, et al. Isovolumic relaxation flow propagation velocity in patients with diseases impairing ventricular relaxation. J Am Soc Echocardiogr 2005;18:221-5.
64. Kanzaki H, Nakatani S, Yamada N, Urayama S, Miyatake K, Kitakaze M. Impaired systolic torsion in dilated cardiomyopathy: reversal of apical rotation at mid-systole characterized with magnetic resonance tagging method. Basic Res Cardiol 2006;101:465-70.

65. Bertini M, Nucifora G, Marsan NA, et al. Left ventricular rotational mechanics in acute myocardial infarction and in chronic (ischemic and nonischemic) heart failure patients. The American journal of cardiology 2009;103:1506-12.
66. Garot J, Pascal O, Diebold B, et al. Alterations of systolic left ventricular twist after acute myocardial infarction. American journal of physiology 2002;282:H357-62.
67. Starr I JWA, Meade R H J. The absence of conspicuous increments of venous pressure after severe damage to the right ventricle of the dog. Am Heart J 1943:26291–300.
68. Burgess MI, Mogulkoc N, Bright-Thomas RJ, Bishop P, Egan JJ, Ray SG. Comparison of echocardiographic markers of right ventricular function in determining prognosis in chronic pulmonary disease. J Am Soc Echocardiogr 2002;15:633-9.
69. Mehta SR, Eikelboom JW, Natarajan MK, et al. Impact of right ventricular involvement on mortality and morbidity in patients with inferior myocardial infarction. Journal of the American College of Cardiology 2001;37:37-43.
70. de Groote P, Millaire A, Foucher-Hossein C, et al. Right ventricular ejection fraction is an independent predictor of survival in patients with moderate heart failure. Journal of the American College of Cardiology 1998;32:948-54.
71. D'Alonzo GE, Barst RJ, Ayres SM, et al. Survival in patients with primary pulmonary hypertension. Results from a national prospective registry. Annals of internal medicine 1991;115:343-9.
72. Uznanska B, Chrzanowski L, Plewka M, Lipiec P, Krzeminska-Pakula M, Kasprzak JD. The relationship between left ventricular late-systolic rotation and twist, and classic parameters of ventricular function and geometry. Kardiologia polska 2008;66:740-7; discussion 8-9.
73. Kim HK, Sohn DW, Lee SE, et al. Assessment of left ventricular rotation and torsion with two-dimensional speckle tracking echocardiography. J Am Soc Echocardiogr 2007;20:45-53.
74. Bansal M, Leano RL, Marwick TH. Clinical assessment of left ventricular systolic torsion: effects of myocardial infarction and ischemia. J Am Soc Echocardiogr 2008;21:887-94.
75. Helle-Valle T, Remme EW, Lyseggen E, et al. Clinical assessment of left ventricular rotation and strain: a novel approach for quantification of function in infarcted myocardium and its border zones. American journal of physiology 2009;297:H257-67.
76. Sun JP, Niu J, Chou D, et al. Alterations of regional myocardial function in a swine model of myocardial infarction assessed by echocardiographic 2-dimensional strain imaging. J Am Soc Echocardiogr 2007;20:498-504.
77. Takeuchi M, Nishikage T, Nakai H, Kokumai M, Otani S, Lang RM. The assessment of left ventricular twist in anterior wall

myocardial infarction using two-dimensional speckle tracking imaging. J Am Soc Echocardiogr 2007;20:36-44.
78. Opdahl A, Helle-Valle T, Remme EW, et al. Apical rotation by speckle tracking echocardiography: a simplified bedside index of left ventricular twist. J Am Soc Echocardiogr 2008;21:1121-8.
79. Takeuchi M, Nakai H, Kokumai M, Nishikage T, Otani S, Lang RM. Age-related changes in left ventricular twist assessed by two-dimensional speckle-tracking imaging. J Am Soc Echocardiogr 2006;19:1077-84.
80. Zhang L, Xie M, Fu M, et al. Assessment of age-related changes in left ventricular twist by two-dimensional ultrasound speckle tracking imaging. J Huazhong Univ Sci Technolog Med Sci 2007;27:691-5.
81. Nagel E, Stuber M, Burkhard B, et al. Cardiac rotation and relaxation in patients with aortic valve stenosis. European heart journal 2000;21:582-9.
82. Wang J, Khoury DS, Yue Y, Torre-Amione G, Nagueh SF. Preserved left ventricular twist and circumferential deformation, but depressed longitudinal and radial deformation in patients with diastolic heart failure. European heart journal 2008;29:1283-9.
83. Sandstede JJ, Johnson T, Harre K, et al. Cardiac systolic rotation and contraction before and after valve replacement for aortic stenosis: a myocardial tagging study using MR imaging. Ajr 2002;178:953-8.
84. Henein MY, O'Sullivan C, Davies SW, Sigwart U, Gibson DG. Effects of acute coronary occlusion and previous ischaemic injury on left ventricular wall motion in humans. Heart (British Cardiac Society) 1997;77:338-45.

Supplements

Table 3. Mean deflection and direction of the rotation axes in 39 subjects.

	angle z		**angle** xy		
BASAL	*mean (SD)*	*95% CI*	*mean (SD)*	*95% CI*	
R-wave	16.8 (11.6)	13.1–20.6	301.4 (106.3)	231.0–11.8	1.3
IVC	15.4 (9.8)	12.2–18.5	14.2 (88.0)	333.9–54.6	3.7*
AVO	17.4 (10.6)	14.0–20.8	17.0 (59.7)	357.3–36.7	13.2**
25% ejection	19.0 (9.8)	15.7–22.2	49.2 (130.4)	235.4–223.0	0.2
50% ejection	24.2 (14.7)	19.2–29.2	226.9 (31.7)	216.6–237.3	26.5***
75% ejection	22.6 (13.0)	18.4–26.8	214.8 (29.1)	205.7–223.9	30.1***
AVC	23.0 (12.5)	19.0–27.1	213.2 (24.5)	205.5–220.8	32.5***
IVR	23.5 (13.3)	19.2–27.8	210.1 (29.5)	200.8–219.3	30.0***
MVO	24.5 (13.7)	20.1–29.0	202.9 (44.3)	189.1–216.6	21.5***
E-peak	26.5 (14.7)	21.6–31.4	197.6 (45.4)	183.1–212.1	19.8***
E-end	22.2 (12.6)	18.1–26.3	224.6 (64.7)	202.1–247.1	10.6***
A-onset	15.8 (9.5)	12.6–18.9	215.4 (62.3)	193.9–236.9	11.3***
MID					
R-wave	9.1 (6.9)	6.9–11.4	358.5 (107.3)	285.7–71.2	1.1
IVC	10.1 (6.1)	8.1–12.0	21.9 (98.7)	326.5–77.3	2.0
AVO	8.5 (5.5)	6.7–10.3	48.7 (100.1)	350.9–106.4	1.8
25% ejection	12.8 (7.1)	10.4–15.1	216.3 (107.3)	142.5–290.2	1.1

50% ejection	14.0 (8.9)	11.0–16.9	224.1 (58.8)	201.8–246.5	10.1***
75% ejection	12.4 (7.2)	10.0–14.7	222.5 (38.1)	210.7–234.3	25.1***
AVC	13.8 (8.3)	11.1–16.5	218.6 (38.3)	205.0–232.1	19.2***
IVR	13.9 (8.9)	10.9–16.7	210.9 (40.4)	198.2–223.6	23.1***
MVO	15.3 (8.4)	12.5–18.0	203.4 (57.4)	184.7–222.0	14.3***
E-peak	15.6 (9.0)	12.6–18.6	206.1 (47.8)	190.8–221.5	18.4***
E-end	12.8 (7.9)	10.2–15.4	203.6 (67.3)	176.2–231.0	7.3***
A-onset	12.4 (6.8)	10.1–14.6	222.6 (78.4)	191.1–254.1	5.9**
APICAL					
R-wave	17.0 (11.8)	13.1–20.8	70.1 (115.5)	333.4–166.8	0.6
IVC	17.6 (12.0)	13.7–21.5	55.7 (106.6)	344.4–127.0	1.2
AVO	16.6 (10.0)	13.3–19.8	217.3 (124.2)	84.3–350.2	0.4
25% ejection	23.0 (11.2)	19.4–26.6	119.1 (119.5)	7.5–230.7	0.5
50% ejection	16.9 (11.6)	13.1–20.6	106.8 (97.0)	46.8–166.8	1.7
75% ejection	13.3 (8.3)	10.6–16.0	134.6 (84.7)	97.8–171.4	4.3*
AVC	13.6 (8.3)	10.8–16.2	142.7 (79.0)	106.7–178.8	4.5**
IVR	17.2 (11.4)	13.5–20.9	149.6 (59.4)	130.0–169.1	13.3***
MVO	18.5 (11.2)	14.9–22.1	146.0 (80.7)	113.0–179.0	5.4**
E-peak	21.4 (12.8)	17.1–25.7	149.9 (82.1)	114.7–185.2	4.7**
E-end	20.0 (13.0)	15.7–24.3	209.3 (68.7)	181.0–237.6	6.9***
A-onset	19.0 (10.7)	15.5–22.5	202.1 (85.6)	163.9–240.4	4.1*

Table 3. Mean deflection ($angle_z$) and direction ($angle_{xy}$) in degrees (SD) and 95 % confidence interval (CI) for the rotation axes at the basal, mid and apical levels measured in 39 healthy subjects at 12 time points during the cardiac cycle. Rayleigh-test was used to test uniformity of the deflection. The Z-values from this test are listed and marked with significant levels ($p \leq 0.05^*$, $p \leq 0.01^{**}$, $p \leq 0.001^{***}$). Ant, anteroseptal; ant, anterior; lat, lateral; post, posterior; inf, inferior; sept, septal; IVC, mid isovolumic contraction; AVO, aortic valve opening; AVC, aortic valve closure; IVR, mid isovolumic relaxation; MVO, mitral valve opening; E-peak, peak of early diastolic filling; E-end, end of early diastolic filling; A-onset, start of atrial wave.

Table 4. Mean deflection, direction and height of the transition plane in 39 healthy subjects.

Transition plane	**angle** z		**angle** xy		
	mean (SD)	*95% CI*	*mean (SD)*	*95% CI*	*z-level (%)*
R-wave	17.3 (11.3)	12.1–22.6	204.2 (107.0)	103.6–304.9	51.7 (20.0)
IVC	12.1 (7.9)	8.7–15.5	318.6 (104.6)	231.6–45.6	61.1 (21.0)
AVO	16.5 (11.4)	11.9–21.1	40.8 (89.8)	348.7–92.8	65.4 (21.5)
25% ejection	20.0 (12.5)	14.7–25.3	213.0 (90.0)	158.6–267.4	58.2 (19.7)
50% ejection	18.7 (10.4)	14.7–22.5	231.5 (66.6) ***	205.1–258.0	62.7 (16.3)
75% ejection	15.9 (9.5)	12.8–19.0	222.8 (39.5) ***	210.4–235.2	65.7 (13.6)
AVC	17.5 (8.8)	14.6–20.4	217.0 (38.0) ***	205.1–229.0	67.1 (10.5)
IVR	19.2 (10.6)	15.8–22.7	208.4 (41.6) ***	195.4–221.5	65.8 (12.4)
MVO	19.8 (10.9)	16.1–23.6	207.4 (56.6) ***	188.1–227.7	68.2 (14.4)
E-peak	21.4 (11.8)	17.0–25.9	194.8 (46.3) ***	178.3–211.3	69.2 (17.5)
E-end	21.8 (14.4)	16.8–26.8	222.0 (75.5) **	191.1–252.9	56.3 (17.6)
A-onset	16.7 (10.3)	13.1–20.4	215.8 (69.6) ***	188.7–243.0	51.6 (17.1)

Table 4. Mean deflection ($angle_z$) and direction ($angle_{xy}$), in degrees (SD) and 95 % confidence interval (CI) for the rotation axis of the transition planes measured in 39 healthy subjects for 12 time points during the cardiac cycle. The column to the right lists the z-level of the transition plane in percent, with apex 0% and basal level = 100%. Significant mean direction (angle xy) by Rayleigh-test is indicated by * *(* = $p<0.05$, ** = $p<0.01$, *** = $p<0.001$)*. Ant, anteroseptal; ant, anterior; lat, lateral; post, posterior; inf, inferior; sept, septal; IVC, mid isovolumic contraction; AVO, aortic valve opening; AVC, aortic valve closure; IVR, mid isovolumic relaxation; MVO, mitral valve opening; E-peak, peak of early diastolic filling; E-end, end of early diastolic filling; A-onset, start of atrial wave.

Table 5. Mean direction of the rotation axis at three levels in 6 pigs at baseline and after 4 minutes of LAD occlusion.

	Apical		**Mid ventricular**		**Basal**	
Time point	Baseline	LAD 4min	Baseline	LAD 4min	Baseline	LAD 4min
R wave	36 (49)	24 (92)	50 (53)	122 (55)	100 (100)	157 (83)
Mid IVC	120 (86)	3 (97)	61 (38)	220 (75) *	190 (65)	127 (131)
AVO	233 (97)	286 (66)	98 (56)	264 (113)	52 (63)	197 (81) *
25% ejection	357 (88)	176 (95) *	199 (61)	54 (71) **	241 (36)	16 (64) **
50% ejection	58 (67)	148 (105)	207 (25)	89 (49) ***	228 (11)	19 (83) **
75% ejection	78 (69)	132 (58)	204 (35)	81 (34) ***	231 (11)	13 (70) **
AVC	79 (67)	75 (45)	208 (28)	78 (38) ***	231 (14)	357 (63) **
Mid IVR	82 (66)	86 (61)	206 (27)	78 (41) ***	235 (20)	345 (82) *
MVO	89 (65)	103 (67)	215 (27)	80 (52) ***	236 (24)	309 (83)
MVO +50 ms	45 (66)	84 (95)	215 (43)	137 (59) *	240 (25)	321 (94)
MVO +100 ms	12 (46)	141 (98)	311 (87)	92 (19) *	192 (94)	336 (98) *

Table 5. Mean and SD of the direction of the rotation axis at three levels and eleven time points in 6 pigs at baseline and after 4 minutes of LAD occlusion.* indicates significant difference between baseline and LAD 4min (* = $p<0.05$, ** = $p<0.01$, *** = $p<0.001$). R wave = beginning of cardiac cycle, Mid IVC = mid isovolumic contraction, AVO/AVC = aortic valve opening/closure, Mid IVR = mid isovolumetric relaxation, MVO = mitral valve opening.